

# **Marine Mammal Monitoring on Navy Ranges (M3R) on the Southern California Offshore Range (SOAR) and the Pacific Missile Range Facility (PMRF) 2017**

DiMarzio, N., Jones, B., Moretti, D., Thomas, L., Oedekoven, C. (2018). "Marine Mammal Monitoring on Navy Ranges (M3R) on the Southern California Offshore Range (SOAR) and the Pacific Missile Range Facility (PMRF)- 2017". Naval Undersea Warfare Center, Newport RI. 34 pp.



DiMarzio, N., Jones, B., Moretti, D., Thomas, L., Oedekoven, C. 2018. Marine Mammal Monitoring on Navy Ranges (M3R) on the Southern California Offshore Range (SOAR) and the Pacific Missile Range Facility (PMRF)- 2017. Prepared for Commander, U.S. Pacific Fleet, Pearl Harbor, HI by Naval Undersea Warfare Center, Newport RI. Work completed under funding document No. N0007018WR4C513 (SOCAL) and funding document No. N0007018WR4C525 (PMRF). 48 pp.

<b>REPORT DOCUMENTATION PAGE</b>		<i>Form Approved</i> <b>OMB No. 0704-0188</b>
Public reporting burden for this collection of information is estimated to average 1 hour per response, including the time for reviewing instructions, searching data sources, gathering and maintaining the data needed, and completing and reviewing the collection of information. Send comments regarding this burden estimate or any other aspect of this collection of information, including suggestions for reducing this burden to Washington Headquarters Service, Directorate for Information Operations and Reports, 1215 Jefferson Davis Highway, Suite 1204, Arlington, VA 22202-4302, and to the Office of Management and Budget, Paperwork Reduction Project (0704-0188) Washington, DC 20503.		
<b>PLEASE DO NOT RETURN YOUR FORM TO THE ABOVE ADDRESS.</b>		
<b>1. REPORT DATE</b> (DD-MM-YYYY) 07-26-2018	<b>2. REPORT TYPE</b> Monitoring report	<b>3. DATES COVERED</b> (From - To) 1 October 2016 - 30 September 2017
<b>4. TITLE AND SUBTITLE</b> M3 MONITORING ON THE SOUTHERN CALIFORNIA OFFSHORE RANGE (SCORE) AND THE PACIFIC MISSILE RANGE FACILITY (PMRF) 2017	<b>5a. CONTRACT NUMBER</b>	
	<b>5b. GRANT NUMBER</b>	
	<b>5c. PROGRAM ELEMENT NUMBER</b>	
	<b>5d. PROJECT NUMBER</b>	
<b>6. AUTHOR(S)</b> Nancy DiMarzio Ben Jones David Moretti Len Thomas Cornelia Oedekoven	<b>5e. TASK NUMBER</b>	
	<b>5f. WORK UNIT NUMBER</b>	
	<b>8. PERFORMING ORGANIZATION REPORT NUMBER</b>	
<b>7. PERFORMING ORGANIZATION NAME(S) AND ADDRESS(ES)</b> Naval Undersea Warfare Center, Newport, RI		<b>10. SPONSOR/MONITOR'S ACRONYM(S)</b>
<b>9. SPONSORING/MONITORING AGENCY NAME(S) AND ADDRESS(ES)</b> Commander, U.S.Pacific Fleet, 250 Makalapa Dr. Pearl Harbor, HI		<b>11. SPONSORING/MONITORING AGENCY REPORT NUMBER</b>
<b>12. DISTRIBUTION AVAILABILITY STATEMENT</b> Approved for public release; distribution is unlimited		
<b>13. SUPPLEMENTARY NOTES</b>		
<b>14. ABSTRACT</b> In 2016, corrected Cuvier's beaked whale ( <i>Ziphius cavirostris</i> , Zc) abundance estimates at SOAR were completed for 2010 -2014. The estimates showed no decline in abundance over this 5-year period on the instrumented Southern California Anti-Submarine Warfare Range (SOAR). In 2017, these estimates were updated with data from 2015 through September of 2017 to provide a yearly estimate from 2010 to 2017. Periods of node or in-water hardware outages in past estimates and new data were isolated. Correction factors for these periods were calculated, and revised abundance estimates were produced. As before, the data do not show a decline in abundance on SOAR over the last eight years.  In 2017, the first extended archive of processed data at PMRF was obtained. Previous data recordings had been restricted to periods (days to weeks) around biannual tests. Six months of continuous data were recorded and analyzed for Blainville's beaked whale ( <i>Mesoplodon densirostris</i> , Md) abundance and added to the previous estimates. No decline in abundance at PMRF is indicated. In parallel, initial data provided by SPAWAR is being used to develop an advanced density estimation algorithm that can account for non-uniform temporal and spatial distributions that are present at SOAR and PMRF, and will allow better estimation of density.  A real-time sonar detector has been incorporated into the M3R software at SOAR and PMRF. Detection reports are produced and integrated into the M3R real-time archives. Currently, precisely time-tagged cetacean detections and localizations and sonar detections are produced and archived in real-time on both SOAR and PMRF. Calibration of the		

SOAR and BSURE hydrophones was undertaken. This provides a means of determining the received level of sonar on the range hydrophones, and will reduce the time required to analyze sonar data in conjunction with cetacean detection data.

Testing of bidirectional nodes as a means of estimating the prey field across the SOAR range was initiated. Prior attempts at prey mapping used a surface [1] or a REMUS deployed echosounder [2]. While these tests provided valuable data, they were of short duration (days). Range bidirectional hydrophones are available on both SOAR and PMRF and may provide the ability to estimate prey density and distribution across the range over broad spatial and temporal scales. The nodes are being evaluated as source/receivers for near-bottom prey mapping. By emitting pings from and receiving echo-returns off prey, it may be possible to monitor prey fields on a scheduled basis over the entire range. This would provide a means of correlating long-term fluctuations in the prey field with changes in beaked whale abundance and distribution.

In concert with passive acoustic monitoring, on-water teams deployed tags and collected biopsy samples at both SOAR and PMRF. At SOAR, four satellite tags were deployed; one each on a Zc and a fin whale (*Balaenoptera physalus*), and two on Risso's dolphins (*Grampus griseus*) [3]. In total, 20 SOAR sightings of Zc have resulted in identification of 56 different individuals [3]. At PMRF, tags were deployed on two rough-toothed dolphins (*Steno bredanensis*), two melon-headed whales (*Peponocephala electra*), and two pantropical spotted dolphins (*Stenella attenuata*) [4].

The tools developed and deployed at SOAR and PMRF allow estimation of beaked whale population trends. However, monitoring the health of the population requires an understanding of sonar usage, the effect of repeated exposure on the animal, and potential environmental changes including those related to the prey field. Obtaining the necessary data will require a coordinated effort and multiple modalities including passive acoustics, visual observation, photographic studies, tags and biological sampling

#### 15. SUBJECT TERMS

Monitoring, passive acoustic monitoring, marine mammals, beaked whales, abundance, Hawaii Range Complex, Southern California Range Complex, Pacific Missile Range Facility, Southern California Offshore Range, mid-frequency active sonar

<b>16. SECURITY CLASSIFICATION OF:</b>			<b>17. LIMITATION OF ABSTRACT</b> UU	<b>18. NUMBER OF PAGES</b> 59	<b>19a. NAME OF RESPONSIBLE PERSON</b> Department of the Navy
<b>a. REPORT</b> Unclassified	<b>b. ABSTRACT</b> Unclassified	<b>c. THIS PAGE</b> Unclassified			<b>19b. TELEPHONE NUMBER (Include area code)</b> 808-471-6391

## Table of Contents

LIST OF FIGURES.....	II
LIST OF TABLES.....	IV
ACRONYMS.....	VI
1.0 EXECUTIVE SUMMARY .....	1
2.0 METHODS.....	2
2.1 SOAR Study Area.....	2
2.2 SOAR Data .....	3
2.3 SOAR Zc Group Analysis.....	5
2.3.1 SOAR Steps to form the Zc groups .....	5
2.3.2 SOAR Autogrouper Detection Statistics .....	5
2.3.3 SOAR Missing Hydrophone Strings & Legacy Hydrophones .....	7
2.3.4 SOAR Zc Abundance.....	14
3.0 SOAR RESULTS.....	15
3.1 SOAR Overview .....	15
3.2 SOAR Dive Starts per Hour Effort .....	16
3.3 SOAR Group Vocal Periods .....	19
3.4 SOAR Zc Clicks per Hour .....	20
3.5 SOAR Abundance.....	23
3.5.1 SOAR Overview.....	23
3.5.2 SOAR Monthly Abundance.....	24
3.5.3 SOAR Yearly Abundance Trends.....	26
3.5.4 SOAR Abundance on a 24-hour cycle.....	27
4.0 ESTIMATING THE SOAR ZC RISK FUNCTION .....	30
4.1 SOAR Data .....	30
4.2 SOAR Analysis.....	30
5.0 SOAR AND BSURE HYDROPHONE CALIBRATION.....	32
5.1 SOAR and BSURE Overview .....	32
5.2 SOAR and BSURE Transfer function estimation.....	33
5.3 SOAR and BSURE Validation using real-world data .....	35
6.0 PMRF STUDY SITE .....	37
6.1 PMRF Overview .....	37
6.2 PMRF abundance.....	37
6.2.1 PMRF Data Summary.....	37
6.2.2 PMRF Abundance.....	40
6.3 PMRF <i>Md</i> behavioral risk function .....	42
7.0 WORKS CITED .....	45
APPENDIX A: SOAR CLICK TRAIN PROCESSOR (CTP) FILE LIST .....	A-46

## List of Figures

Figure 1. SOAR hydrophone range, showing the M3R MMAMMAL display on the left, and the M3R World Wind display on the right.....	2
Figure 2. Rating of clicks: (a) Confidence = 1 Zc clicks, (b) Confidence = 2 Zc clicks, (c) delphinid clicks.....	6
Figure 3. SOAR range showing the legacy hydrophones (<100) and the newer hydrophone strings (100-900).....	9
Figure 4. Dive start GVPs for each year along with effort start (green) and effort stop (red) times indicated with vertical lines. Effort start and stop times were calculated by finding gaps in effort greater than 24 hours. ....	15
Figure 5. Mean monthly number of dive starts per hour effort, averaged across 2010 to 2017. ....	16
Figure 6. Mean monthly number of dive starts per hour effort for 2010 to 2017.....	17
Figure 7. Number of dive starts per hour averaged across 2010-2017 for every hour of the year, along with 1st to 4th order fits to the data. The 4th order fit used to correct the dive start data is shown in yellow.....	18
Figure 8. Mean number of Zc dive starts per hour on a 24-hour cycle. Note that the times are in UTC, and the gray shaded area indicates the approximate local night hours, if local day is considered 7a to 7p, and local night is considered 7p to 7a. There is a 7 or 8-hour difference between local time on San Clemente Island and UTC, depending on Daylight Savings Time... 18	18
Figure 9. SOAR corrected mean monthly Zc group vocal period (GVP), averaged across 2010-2017. ....	19
Figure 10. SOAR corrected mean monthly Zc group vocal period (GVP) for 2010 through 2017.....	20
Figure 11. Corrected mean monthly number of Zc clicks detected per hour, averaged across 2010-2017. ....	21
Figure 12. Corrected mean monthly number of Zc clicks detected per hour for the years 2010 through 2017.....	21
Figure 13. Number of clicks detected per hour across the range averaged across 2010-2017 for every hour of the year, along with 1st to 4th order fits to the data. The 4th order fit used to correct the dive start data is shown in yellow.....	22
Figure 14. Mean number of Zc clicks detected per hour on the range on a 24-hour cycle. Note that the times are in UTC, and the gray shaded area indicates the approximate local night hours, if local day is considered 7a to 7p, and local night is considered 7p to 7a. There is a 7 or 8-hour difference between local time on San Clemente Island and UTC, depending on Daylight Savings Time. ....	22
Figure 15. Corrected mean monthly abundance at SOAR, averaged between 2010 and 2017. ....	24
Figure 16. Corrected mean monthly Zc abundance for the years 2010-2017.....	25
Figure 17. Corrected mean monthly abundance for the month of December, 2010-2017.....	26
Figure 18. Corrected mean Zc abundances by month, from year 2010-2017.....	27
Figure 19. Abundance per hour averaged across 2010-2017 for every hour of the year, along with 1st to 4th order fits to the data. The 4th order fit used to correct the dive start data is shown in yellow. ....	28
Figure 20. Mean Zc abundance per hour on a 24-hour cycle. Note that the times are in UTC, and the gray shaded area indicates the approximate local night hours, if local day is considered 7a to 7p, and local night is considered 7p to 7a. There is a 7 or 8-hour difference between local time on San Clemente Island and UTC, depending on Daylight Savings Time.....	29
Figure 21. Data acquisition system block diagram.....	33
Figure 22. Test system block diagram.....	34

Figure 23. The relationship between the predicted sound pressure level (SPL) from the MK 30 positions and propagation model are plotted as a function of the predictions from the laboratory validation. The colored dots depict the data with color indicating the hydrophone that detected the MK 30 ping. The black dots indicate the median value for each hydrophone and the white diagonal line in the background is a 1-1 line. The rug plots along the horizontal and vertical axis depict the projection of the data point onto that axis. .... 36

Figure 24. An outline of the PMRF range on the right. The PMRF range boundaries are indicated by the outer red line. The BARSTUR range area is indicated by the inner red line. The left plot shows the distribution of beaked whale click detections. The dots represent the range hydrophones including those in SWTR. .... 37

Figure 25. PMRF *Md* dive start GVPs for 2015 along with effort start (green) and effort stop (red) times indicated with vertical lines. Effort start and stop times were calculated by finding gaps in effort greater than 24 hours. .... 38

Figure 26. PMRF *Md* dive start GVPs for 2016 along with effort start (green) and effort stop (red) times indicated with vertical lines. Effort start and stop times were calculated by finding gaps in effort greater than 24 hours. .... 39

Figure 27. PMRF *Md* dive start GVPs for 2017 along with effort start (green) and effort stop (red) times indicated with vertical lines. Effort start and stop times were calculated by finding gaps in effort greater than 24 hours. .... 39

Figure 28. Mean PMRF *Md* abundance per year from 2015-2017. .... 40

Figure 29. Mean monthly *Md* abundance for years 2015-2017. .... 41

Figure 30. Daily *Md* abundance for the month of February 2017 in black (dotted lines = 95% CI). Detections from the sonar detector for all range hydrophone are presented by the colored bars. .... 42

Figure 31. Locations (jittered) of the 62 hydrophones included in the SPAWAR dataset, with simple tessellation tiles on the left and improved tiles (assuming a 6.5km effective detection radius) on the right. .... 43

Figure 32. Partial fit plots for smooths from binomial GAM, on the scale of the logistic link function. The 2-dimensional spatial smooth term  $s(\text{Longitude}, \text{Latitude})$  is illustrated in the heat plot showing a 2-D spatial smooth with hydrophone locations. Contour lines in heat plots represent surfaces at  $\pm 0.5, 1, 1.5$  standard errors. Vertical lines in the smooth for covariates depth and Julian date indicate locations of observations. .... 44

## List of Tables

Table 1. The number of days per month on which archives were collected at SOAR with the CS-SVM classifier. The CS-SVM <i>Zc</i> foraging click classifier was installed in May, 2010 (blue) and the CS-SVM <i>Zc</i> buzz click classifier was installed in July, 2014 (pink). FFT-based detections (Whdetect) have been collected at SOAR since 2006.....	3
Table 2. Click types for the full-bandwidth FFT-based energy detector. ....	4
Table 3. CS-SVM classes at SOAR from May, 2010 to May, 2014 .....	4
Table 4. CS-SVM classes at SOAR as of May, 2014 .....	4
Table 5. AutoGrouper detection statistics and correction factors for <i>Zc</i> in SOAR.....	7
Table 6. Number of <i>Zc</i> groups detected for various Autogrouper configurations for the sample data from 2012-2016. ....	9
Table 7. Ratios of the number of <i>Zc</i> groups detected in Table 6 for the various Autogrouper configurations to the Autogrouper run with all hydrophones. CF (the means of the ratios across years 2012 – 2016) indicates the correction factors derived for the number of <i>Zc</i> group dive starts.....	10
Table 8. Mean Group Vocal Periods (GVPs) for various Autogrouper configurations for the sample data from 2012-2016. ....	10
Table 9. Ratios of mean Group Vocal Periods (GVPs) in Table 8 for the various Autogrouper configurations to the Autogrouper run with all hydrophones. CF (the means of the ratios across years 2012 – 2016) indicates the correction factors derived for the GVPs. ....	11
Table 10. Mean group click count for various Autogrouper configurations for the sample data from 2012-2016.....	11
Table 11. Ratios of mean group click counts in Table 10 for the various Autogrouper configurations to the Autogrouper run with all hydrophones. CF (the means of the ratios across years 2012 – 2016) indicates the correction factors derived for the group click counts.....	11
Table 12. Number of <i>Zc</i> groups detected for the samples in each year, for all hydrophones, and for Legacy hydrophones removed.....	12
Table 13. Ratios of the number of <i>Zc</i> groups detected in Table 12 when Legacy hydrophones are removed to the number detected when Legacy hydrophones are included. CF (the ratio of the total number of groups detected without Legacy hydrophones to the total detected with Legacy hydrophones, for all sample years) indicates the correction factor derived for the number of <i>Zc</i> group dive starts.....	12
Table 14. <i>Zc</i> mean Group Vocal Periods (GVPs) for the samples in each year, for all hydrophones, and for Legacy hydrophones removed. ....	13
Table 15. Ratios of the <i>Zc</i> mean GVPs in Table 14 when Legacy hydrophones are removed to the GVPs when Legacy hydrophones are included. CF (the means of the ratios across all sample years) indicates the correction factor derived for the GVPs.....	13
Table 16. <i>Zc</i> mean number of clicks detected per group for the samples in each year, for all hydrophones, and for Legacy hydrophones removed.....	13
Table 17. Ratios of the <i>Zc</i> mean number of clicks detected per group in Table 16 when Legacy phones are removed to the mean group click counts when Legacy phones are included. CF (the means of the ratios across the sample years) indicates the correction factor derived for the group click counts.....	13
Table 18. Total number of hours of effort per year in which data was recorded.....	15
Table 21. Mean monthly # dive starts per hour effort, averaged across 2010 to 2017 .....	16
Table 22. Monthly CVs for the mean number of dive starts per hour effort, 2010 to 2017 .....	16
Table 23: SOAR corrected monthly mean number of <i>Zc</i> group dive starts for 2010 to 2017 .....	17



Table 24. SOAR mean monthly corrected *Zc* group vocal periods (GVPs) for 2010 to 2017, and average across 2010-2017. NAs indicate missing data. .... 19

Table 25. SOAR mean monthly number of corrected *Zc* clicks per hour for 2010 to 2017, and average across 2010-2017. NAs indicate missing data. .... 20

Table 26. Total number of dive starts (*n<sub>d</sub>*) per month for 2010-2017 at SOAR. NAs indicate missing data..... 23

Table 27. Total measurement time period per month, or total number of hours of effort per month (T), for years 2010-2017. NAs indicate missing data..... 23

Table 28. Mean monthly abundances at SOAR averaged over 2010-2017, with CIs calculated using a  $CV = 0.71$ ..... 24

Table 29. Mean monthly SOAR abundances for 2010 - 2017. NAs indicate periods without data. . 25

Table 30. Mean December abundance from 2010 - 2016, with CIs calculated using a  $CV = 0.71$ .... 26

Table 31: Mean monthly *Md* abundance for PMRF, 2015-2017. NAs indicate missing data. ....**Error!**

**Bookmark not defined.**

Table 32: SOAR Click Train Processor (CTP) files from 2010 to 2017. ....A-4

## Acronyms

AUTEC	Atlantic Undersea Test and Evaluation Center
A/D	Analog to Digital
AG	Auto-Grouper
ASP	Acoustic Signal Processor
ASW	Anti-Submarine Warfare
BSURE	Barking Sands Underwater Range Expansion
CF	Correction Factor
CS-SVM	Class-Specific Support Vector Machine classifier (also called SVMJ)
CTF	Cable Termination Facility
CTP	Click Train Processor
CW	Continuous Wave
DIACAP	Defense Information Assurance Certification and Accreditation
DSP	Digital Signal Processor
FA	False Alarm
FFT	Fast Fourier Transform
FN	False Negative
FP	False Positive
GAM	Generalized Additive Model
I/A	Information Assurance
ICI	Inter-Click Interval
M3R	Marine Mammal Monitoring on Navy Ranges
<i>Md</i>	<i>Mesoplodon densirostris</i> , Blainville's beaked whale
MFAS	Mid-Frequency Active Sonar
PCAD	Population Consequences of Acoustic Disturbance
PD	Probability of Detection
PMRF	Pacific Missile Range Facility
$RL_{rms}$	Received Level root mean squared
RMF	Risk Management Framework
SCI	San Clemente Island
SES	Shore Electronics System
SOAR	Southern California Anti-Submarine Warfare Range
SPC	Signal Processor Controller
SVMJ	Jarvis Support Vector Machine classifier (formally CS-SVM)
TDOA	Time Difference of Arrival
TRR	Test Readiness Review
$V_{rms}$	Root mean squared volts
<i>Zc</i>	<i>Ziphius cavirostris</i> , Cuvier's beaked whale

## 1.0 Executive Summary

In 2016, corrected Cuvier's beaked whale (*Ziphius cavirostris*, *Zc*) abundance estimates at SOAR were completed for 2010 -2014. The estimates showed no decline in abundance over this 5-year period on the instrumented Southern California Anti-Submarine Warfare Range (SOAR). In 2017, these estimates were updated with data from 2015 through September of 2017 to provide a yearly estimate from 2010 to 2017. Periods of node or in-water hardware outages in past estimates and new data were isolated. Correction factors for these periods were calculated, and revised abundance estimates were produced. As before, the data do not show a decline in abundance on SOAR over the last eight years.

In 2017, the first extended archive of processed data at PMRF was obtained. Previous data recordings had been restricted to periods (days to weeks) around biannual tests. Six months of continuous data were recorded and analyzed for Blainville's beaked whale (*Mesoplodon densirostris*, *Md*) abundance and added to the previous estimates. No decline in abundance at PMRF is indicated. In parallel, initial data provided by SPAWAR is being used to develop an advanced density estimation algorithm that can account for non-uniform temporal and spatial distributions that are present at SOAR and PMRF, and will allow better estimation of density.

A real-time sonar detector has been incorporated into the M3R software at SOAR and PMRF. Detection reports are produced and integrated into the M3R real-time archives. Currently, precisely time-tagged cetacean detections and localizations and sonar detections are produced and archived in real-time on both SOAR and PMRF. Calibration of the SOAR and BSURE hydrophones was undertaken. This provides a means of determining the received level of sonar on the range hydrophones, and will reduce the time required to analyze sonar data in conjunction with cetacean detection data.

Testing of bidirectional nodes as a means of estimating the prey field across the SOAR range was initiated. Prior attempts at prey mapping used a surface [1] or a REMUS deployed echosounder [2]. While these tests provided valuable data, they were of short duration (days). Range bidirectional hydrophones are available on both SOAR and PMRF and may provide the ability to estimate prey density and distribution across the range over broad spatial and temporal scales. The nodes are being evaluated as source/receivers for near-bottom prey mapping. By emitting pings from and receiving echo-returns off prey, it may be possible to monitor prey fields on a scheduled basis over the entire range. This would provide a means of correlating long-term fluctuations in the prey field with changes in beaked whale abundance and distribution.

In concert with passive acoustic monitoring, on-water teams deployed tags and collected biopsy samples at both SOAR and PMRF. At SOAR, four satellite tags were deployed; one each on a *Zc* and a fin whale (*Balaenoptera physalus*), and two on Risso's dolphins (*Grampus griseus*) [3]. In total, 20 SOAR sightings of *Zc* have resulted in identification of 56 different individuals [3]. At PMRF, tags were deployed on two rough-toothed dolphins (*Steno bredanensis*), two melon-headed whales (*Peponocephala electra*), and two pantropical spotted dolphins (*Stenella attenuata*) [4].

The tools developed and deployed at SOAR and PMRF allow estimation of beaked whale population trends. However, monitoring the health of the population requires an understanding of sonar usage, the effect of repeated exposure on the animal, and potential environmental changes including those related to the prey field. Obtaining the necessary data will require a coordinated effort and multiple modalities including passive acoustics, visual observation, photographic studies, tags and biological sampling.

## 2.0 Methods

### 2.1 SOAR Study Area

The U.S. Navy's Southern California Anti-Submarine Warfare Range (SOAR) is located in the San Nicolas Basin, west of San Clemente Island (SCI), CA. SCI is one of the Channel Islands in the southern California Bight. SOAR is an Anti-submarine Warfare (ASW) training range on which sound sources, including Mid-frequency active sonar (MFAS), are routinely used, and  $Z_c$  are regularly detected acoustically and visually, displaying a high level of site fidelity to the area [5] [6] [7].

The SOAR range consists of an array of 178 bottom-mounted hydrophones covering an area of about 1800 km<sup>2</sup> (Figure 1). The SOAR hydrophone baselines range from about 2.5 to 6.5 km, and are at average depths of 1600-1800 m. The original 88 hydrophones have a bandwidth of ~8 to 40 kHz, while the newer 89 hydrophones have a bandwidth of ~50 Hz to 48 kHz [8].

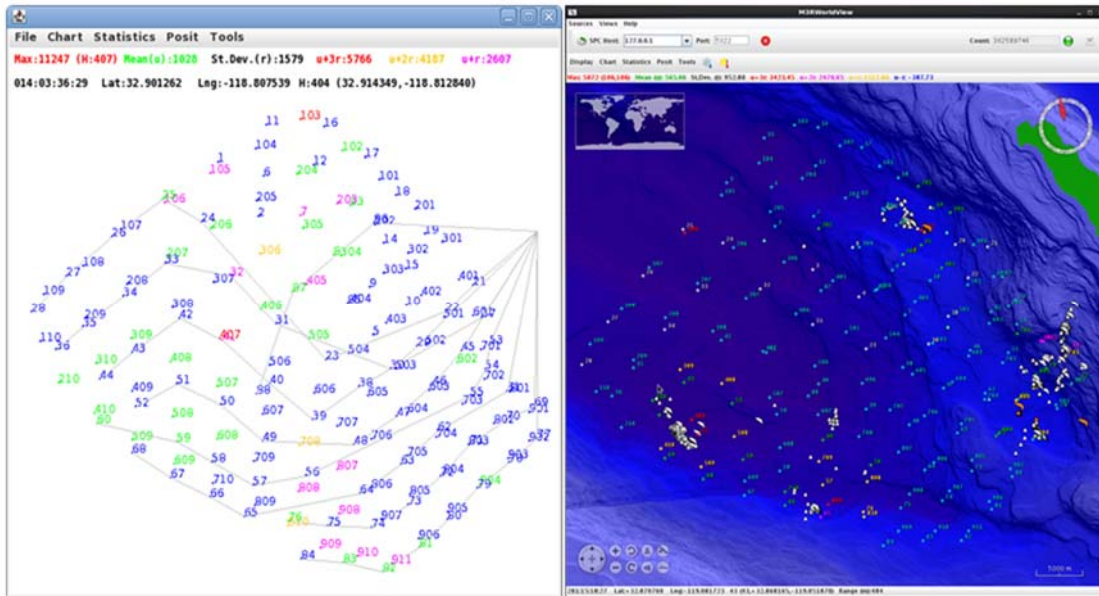


Figure 1. SOAR hydrophone range, showing the M3R MMAMMAL display on the left, and the M3R World Wind display on the right.

## 2.2 SOAR Data

In 2006 the Marine Mammal Monitoring on Navy Ranges (M3R) program installed a real-time passive acoustic system to automatically detect, classify and localize marine mammals using the SOAR hydrophones. Binary archives of detection, classification, and localization data are usually collected continuously year-round, unless there is an operation with a classification that precludes it. At times the system was inadvertently not restarted or the hard disk was damaged, producing the time periods without data. Raw acoustic recordings are collected periodically.

The system primarily uses two types of detectors: an FFT-based spectral energy detector (called 'Whdetect') and a class-specific support vector machine (CS-SVM) classifier [9, 8].

shows the number of days per month on which archives with CS-SVM detections have been collected at SOAR between 2010 and 2017.

M3R SOAR Detection Archives												
	Jan	Feb	Mar	Apr	May	Jun	Jul	Aug	Sep	Oct	Nov	Dec
<b>2010</b>					7			9	30	29	22	23
<b>2011</b>	22	27	8	3	13		6	28	30	31	22	31
<b>2012</b>	27	23	18	30	15	6	1	4		17	13	10
<b>2013</b>					17	30	24	31	30	6	2	12
<b>2014</b>	31	22	28	29	28	17	14	17	28	14	4	31
<b>2015</b>	31	28	24	25	31	15	22	21	15	30	15	11
<b>2016</b>	31	27	31	25	18	7	16	31	27		26	22
<b>2017</b>	15		13	17	2		12	31	24	17	29	10+

**Table 1.** The number of days per month on which archives were collected at SOAR with the CS-SVM classifier. The CS-SVM *Zc* foraging click classifier was installed in May, 2010 (blue) and the CS-SVM *Zc* buzz click classifier was installed in July, 2014 (pink). FFT-based detections (Whdetect) have been collected at SOAR since 2006.

There are two versions of the FFT-based energy detector: full-bandwidth (0-48 kHz) and a low-frequency (0-3 kHz) version added in 2010. Each compares the bins of the FFT to the noise-varying background, sets each bin to '0' (below threshold) or '1' (above threshold), and outputs a detection report with a binary FFT.

The full-bandwidth FFT detector then separates the output into 'clicks' (if at least 10 bins are set to 1) or 'whistles' for further processing. Clicks are classified into types 1 through 5 by finding the frequency band with the most energy (Table 2).

Frequency Band (kHz)	Type	"Class"
45 - 48	1	high frequency
24 - 48	2	beaked whale
12 - 48	3	delphinid
1.5 - 18	4	sperm whale
0 - 1.5	5	low frequency

**Table 2. Click types for the full-bandwidth FFT-based energy detector.**

The CS-SVM classifier, installed in May, 2010, provides robust real-time, automated detection and classification of clicks from several types of odontocetes [5]. When initially installed at SOAR the CS-SVM had six classes (Table 3). As of May, 2014 the dolphin classes 3, 4, and 6 were combined into a 'generalized dolphin' (GD) class (8); the *Zc* buzz (52) class was added [10]; and *Md* was removed, as they are not present on SOAR. Therefore, CS-SVM at SOAR currently has four classes (Table 4). A detection report is generated for each CS-SVM detection. The *Zc* groups identified for this analysis are generated from CS-SVM *Zc* foraging click detections.

Species				
Class	Class	Scientific Name	Common Name	Description
1	<i>Md</i>	<i>Mesoplodon densirostris</i>	Blainville's beaked whale	foraging click
2	<i>Zc</i>	<i>Ziphius cavirostris</i>	Cuvier's beaked whale	foraging click
3	<i>Gm</i>	<i>Globicephala macrorhynchus</i>	pilot whale	click
4	<i>Gg</i>	<i>Grampus griseus</i>	Risso's dolphin	click
5	<i>Pm</i>	<i>Physeter macrocephalus</i>	sperm whale	foraging click
6	<i>Sa</i>	<i>Stenella attenuata</i>		click

**Table 3. CS-SVM classes at SOAR from May, 2010 to May, 2014**

Species/Family				
Class	Class	Scientific Name	Common Name	Description
2	<i>Zc</i>	<i>Ziphius cavirostris</i>	Cuvier's beaked whale	foraging click
5	<i>Pm</i>	<i>Physeter macrocephalus</i>	sperm whale	foraging click
8	GD	delphinidae	generalized dolphin	click
52	<i>Zc</i>	<i>Ziphius cavirostris</i>	Cuvier's beaked whale	buzz click

**Table 4. CS-SVM classes at SOAR as of May, 2014**

## **2.3 SOAR *Zc* Group Analysis**

### **2.3.1 SOAR Steps to form the *Zc* groups**

Software tools have been developed to automatically process the large amounts of M3R archive data and localize groups of diving *Zc*. Several steps are involved in automatically identifying these groups. Small groups of *Zc* appear to dive synchronously, typically vocalizing only below 400 m depth during deep foraging dives [11, 12]. The echolocation clicks during deep foraging dives are first detected and classified as *Zc*, then they are formed into click trains, and finally the clicks trains are associated into *Zc* groups.

For this analysis, only foraging clicks generated by the CS-SVM classifier were used. For each foraging click detection CS-SVM generates a detection report which includes a time stamp, the hydrophone, and a quality factor which indicates the strength of the classification.

A Java-based click train processor (CTP) program then forms the *Zc* click detections into click trains on a per hydrophone basis. A click train is initiated when a click is detected, and clicks are added to the click train until at least three minutes pass without detections. At this point if the click train has at least five clicks a click train report is generated; otherwise the click train is discarded. Click train reports include the hydrophone, the click train start and stop times, the total number of clicks in the click train, and the inter-click interval (ICI).

A Matlab-based Autogrouper (AG) program then uses a set of rules based on time and location of the click trains to associate the CTP click trains into individual groups of vocalizing *Zc*. Only click trains with  $ICI \geq 0.35$  sec and  $ICI \leq 0.75$  sec and with duration greater than 1 min and less than 60 min are used in the grouping process. Locations are based on the hydrophone locations, with the *Zc* group center being the hydrophone with the highest click density (number of clicks per min). To form a *Zc* group the click trains must be within 9.75 km of the group center and the duration of the *Zc* group vocal period must be less than one hour.

### **2.3.2 SOAR Autogrouper Detection Statistics**

Detection statistics for the Autogrouper were derived by comparing the output to a manual review of a set of systematic random samples of the data. The *Zc* groups determined by manual review were considered “truth,” and the probability of detection (PD), percent of false-negatives (FNs), and percent of false-positives (FPs), and FN and FP correction factors were calculated for the AG program.

#### **2.3.2.1 SOAR Manual Review**

One hundred systematic random 1-hour samples were identified between 2010 and 2015, and 31 of these random samples were manually reviewed for the presence of *Zc*. *Zc* group dive starts, i.e., group dives that began within the one-hour sample period, were used for the analysis. A two-step process was used to manually identify the *Zc* group dive starts. First, all range hydrophones were manually reviewed for the potential presence of *Zc* foraging clicks. The start times of the *Zc* click-trains were noted, and a confidence level of 1 or 2 was assigned. A “1” represented a high confidence the click was from *Zc*, and “2” a possibility the clicks may either be delphinid (in particular Risso’s dolphin),

or a combination of *Zc* and delphinid. Figure 2 shows the difference between (a) high-confidence *Zc* clicks; (b) lower-confidence *Zc* clicks, which are either *Zc* with dolphins, or possibly just dolphins; and (c) clicks which are clearly delphinid.

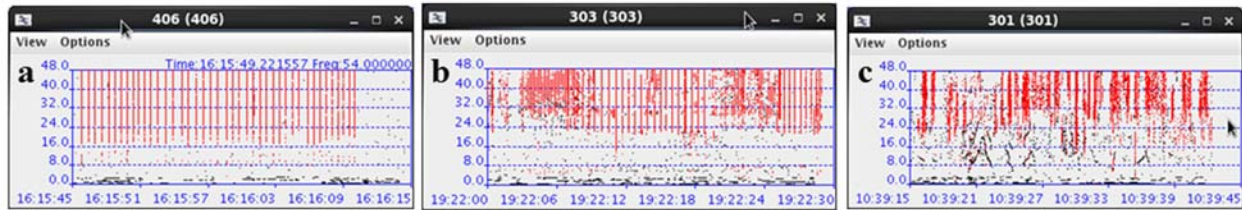


**Figure 2. Rating of clicks: (a) Confidence = 1 *Zc* clicks, (b) Confidence = 2 *Zc* clicks, (c) delphinid clicks**

After all hydrophones were reviewed, those identified in the first pass as potentially *Zc* were plotted on a map of the range, and formed into groups based on the temporal and spatial overlap of the click-trains. A group typically included hydrophones within a baseline of the hydrophone with the highest click density, and with a group vocal period of less than one hour. At times neighboring groups ensounded some common hydrophones. The *Zc* groups that were formed contained exclusively or mostly high confidence *Zc* clicks.

At the conclusion of the second pass the number of dive starts, along with start and stop times of the hydrophones belonging to each group's dive start, were recorded for each of the samples.

### 2.3.2.2 SOAR Autogrouper Algorithm (AG)

The Autogrouper algorithm was run on the output of the CTP program. Echolocation click classes of both *Md* and *Zc* were combined as *Zc* because *Md* are not present at SOAR, and only detections with ICI between 0.35 and 0.75 sec were analyzed. Prior to comparison with the manual groups, the AG output was filtered so that all *Zc* groups had to have a total number of clicks between 300 and 43,200, and a group vocal period (GVP) between 5 and 90 minutes. The minimum number of 300 detected clicks is derived from an ICI of 0.5 sec for 2.5 minutes for one animal, and the maximum of 43,200 is from an ICI of 0.5 sec for six animals for one hour.

### 2.3.2.3 SOAR Comparison of Manual and AG Dive Starts

For each sample the manual and AG dive starts were placed into one of four categories: (a) exact matches, (b) 'confused' matches, (c) manual only (false negatives, FN), or (d) AG only (false positives, FP). A group was considered an exact match if: (1) the groups had at least one hydrophone in common, (2) the hydrophones were not part of another group, and (3) the time periods overlapped. The "confused" matches occurred when all or some of the same hydrophones were identified by both the manual process and the AG program, and the time periods overlapped, but the number of groups and/or the hydrophone combinations forming the groups were not the same.

### 2.3.2.4 SOAR Derivation of Detection Statistics and Correction Factors

Detection statistics were then calculated from the 31 random samples, for all samples combined. Correction factors were also calculated to derive the 'true' number of *Zc* group dive starts present from the number of AG groups detected. The PD was calculated as the number of dive starts correctly detected by the AG divided by the number of manual dive starts. The percentage of FNs (dive starts missed by the AG) was the number of FNs divided by the number of manual dive starts; and the



percentage of FPs (dive starts misidentified by the AG) was the number of FPs divided by the number of AG dive starts.

FP and FN correction factors for the AG dive start results were then derived as follows, using all samples combined:

1. The FP correction factor =  $1 - (\text{number of FP} / \text{number of AG dive starts})$
2. The FN correction factor =  $1 + (\text{number of FN} / (\text{number of AG dive starts} * \text{FP correction factor}))$ .

The detection statistics were considered for two cases: for all group dive starts within the sample hour, and for all group dive starts within the sample hour except “edge-only” cases. The “edge-only” cases are those groups that only contain hydrophones on the edge of the range. These are removed as it is likely that the associated group occurs outside the range boundary. If either the AG or the manual analysis reported an “edge-only” group, both this group and its matching group in the alternate method were removed from the analysis. The detection statistics and correction factors are reported in Table 5.

AutoGrouper case	n	Probability of Detection (PD)	% False Negative (FN)	% False Positive (FP)	Correction Factors	
					FP	FN
all groups	31	0.738	0.262	0.173	0.827	1.355
no edge only groups	31	0.759	0.241	0.185	0.815	1.318

**Table 5. AutoGrouper detection statistics and correction factors for Zc in SOAR.**

### 2.3.3 SOAR Missing Hydrophone Strings & Legacy Hydrophones

#### 2.3.3.1 SOAR Overview

Zc groups are identified from Autogrouper output, which is generated from Click Train Processor (CTP) output, which in turn is run on the binary archive files. The archiver program is called spc archive, where ‘spc’ refers to a signal processor server process where the name, spc, is “NBI”; nothing but initials. The spc archive program creates binary archives of detections, time difference of arrivals (TDOAs), and localizations. Each time the spc archiver is started a unique filename is created, and the archiver automatically opens a new file in the series when the file reaches a certain size. Thus every time the spc archiver is started a new archive series is created, which could consist of anywhere from one to several thousand files. The CTP program has been run on each archive series, so that one CTP file is generated for each archive series. Appendix A lists all of the click train processor (CTP) files from 2010 to 2017 that were used to generate Zc groups.

In the course of data analysis, it was found that CS-SVM, at different times, was not running on certain hydrophones. This could have been due either to the hydrophone string being ‘down’ (not functional) or the algorithm not running on particular hydrophones. In addition, during some periods the CS-SVM was only run on the newer hydrophones (strings 100 through 900), and at other times it was also run on the legacy hydrophones (hydrophones < 100). The list in Appendix A includes whether CS-SVM detections were present from the legacy hydrophones, and whether the algorithm was not detected on any hydrophones in one or more of the newer strings.

In order to account for these inconsistencies, correction factors for both the missing hydrophone strings and for the additional legacy hydrophones were derived to apply to the abundance counts. Different correction factors were also generated from the same data samples for the group vocal periods (GVPs) and the click counts per group. The baseline data was considered to be the case in which CS-SVM was running on all the newer hydrophone strings, but not on the legacy hydrophones. Therefore, the correction factors were applied to normalize the data to the baseline case.

Since the *Zc* groups are generated from the Autogrouper program, the corrections are not simply a case of accounting for missing hydrophones, as a group that contained some of the missing hydrophones could still be present, but comprised of a different hydrophone combination. Therefore, the correction factors were derived by selecting sample 'baseline' archive series, and rerunning the Autogrouper with the various string combinations removed. The ratios of groups calculated with all hydrophones to groups calculated with certain strings removed were then generated. Samples were taken from across different years to compare the consistency of the ratios. Similarly, for the additional legacy hydrophones, a correction factor was calculated from sample archives that included legacy phones. The ratio of the total number of groups detected to the number detected when the legacy phones were removed was used as the correction factor. The samples used for the 'missing hydrophone strings' case are highlighted in yellow in the CTP list in Appendix A, and those used for the 'legacy hydrophone' case are highlighted in pink.

### **2.3.3.2 SOAR Missing Hydrophone Strings**

#### ***2.3.3.2.1 SOAR Data Samples***

In order to calculate correction factors (CF) for the missing hydrophone strings, sample data from the years 2012 through 2016 were reprocessed through the Autogrouper for the various configurations of missing strings. The same sample data were used to find correction factors for the number of *Zc* groups detected, the GVPs, and the number of clicks detected per *Zc* group.

#### ***2.3.3.2.2 SOAR Correction Factors for Number of Zc Groups (Dive Starts)***

Table 6 lists the number of *Zc* groups detected from the sample data for each configuration, by year. It also lists the means across all years and the total number of groups detected across all years ('sums') for the various configurations. The number of groups detected decreases as the number of hydrophone strings removed increases, as would be expected. *Zc* groups are found more often towards the western side of the range, so it seems reasonable that the mean number of groups detected with the 100 string removed is lower than the mean number of groups with the 700 or 900 string removed (Figure 3).

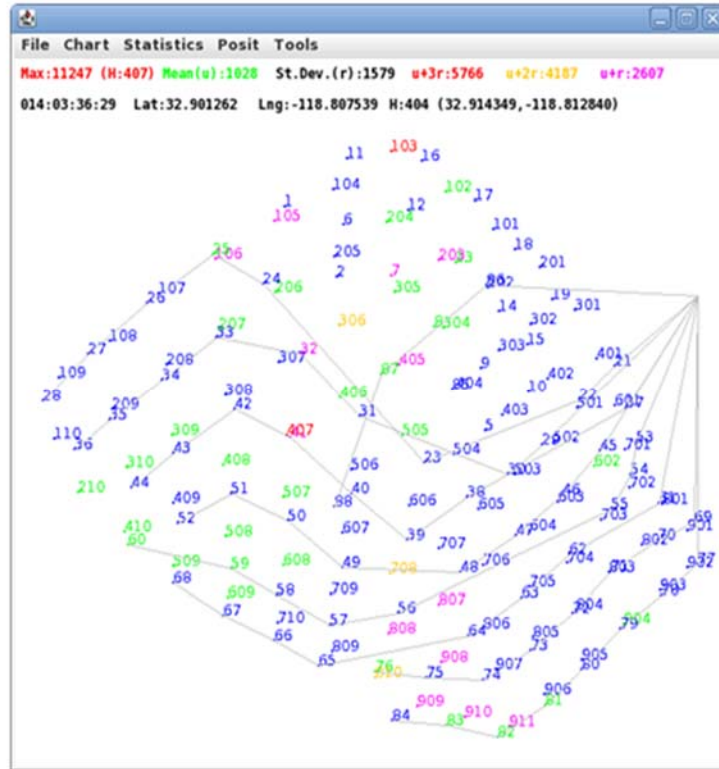


Figure 3. SOAR range showing the legacy hydrophones (<100) and the newer hydrophone strings (100-900).

	2012	2013	2014	2015	2016	means	sums
allhyd	1448	2190	7673	5899	7855	5013.00	25065
no100s	1177	1857	6591	5180	6996	4360.20	21801
no700s	1358	2057	7174	5449	7281	4663.80	23319
no900s	1367	2006	6935	5270	6999	4515.40	22577
no100s900s	1096	1673	5853	4551	6140	3862.60	19313
no100s600s700s	981	1561	5460	4204	5628	3566.80	17834
no600s_to_900s	1067	1511	4914	3501	4501	3098.80	15494

Table 6. Number of Zc groups detected for various Autogrouper configurations for the sample data from 2012-2016.

Ratios were calculated from Table 6 of the number of *Zc* groups detected with hydrophones missing to the number detected using all hydrophones. These ratios are shown in Table 7. The ratios are fairly consistent across the sample years. The means of the ratios across all years were used as correction factors for the corresponding archive series.

	2012	2013	2014	2015	2016	CF (means)
<b>no100s / allhyd</b>	0.81	0.85	0.86	0.88	0.89	0.86
<b>no700s / allhyd</b>	0.94	0.94	0.93	0.92	0.93	0.93
<b>no900s / allhyd</b>	0.94	0.92	0.90	0.89	0.89	0.91
<b>no100s900s / allhyd</b>	0.76	0.76	0.76	0.77	0.78	0.77
<b>no100s600s700s / allhyd</b>	0.68	0.71	0.71	0.71	0.72	0.71
<b>no600s to 900s / allhyd</b>	0.74	0.69	0.64	0.59	0.57	0.65

**Table 7. Ratios of the number of *Zc* groups detected in Table 6 for the various Autogrouper configurations to the Autogrouper run with all hydrophones. CF (the means of the ratios across years 2012 – 2016) indicates the correction factors derived for the number of *Zc* group dive starts.**

### ***2.3.3.2.3 SOAR Correction Factors for the Group Vocal Periods (GVPs)***

The mean GVPs per year for the different hydrophone string combinations are shown in Table 8, along with the means across all years. Using these data, the ratios were calculated of the mean GVPs with missing hydrophones to the mean GVPs when all hydrophones were present (Table 9). The means across all years of these ratios were used as correction factors for the corresponding archive series. The GVPs are very consistent, resulting in correction factors between 0.98 and 1.00.

	2012	2013	2014	2015	2016	Means
<b>allhyd</b>	37.68	32.69	37.94	38.31	37.24	36.77
<b>no100s</b>	37.31	32.76	37.69	38.35	37.41	36.71
<b>no700s</b>	37.60	32.27	37.72	37.86	36.57	36.40
<b>no900s</b>	37.78	32.36	37.63	37.99	36.92	36.54
<b>no100s900s</b>	37.42	32.37	37.30	37.98	37.07	36.43
<b>no100s600s700s</b>	36.96	32.31	37.35	37.53	36.63	36.16
<b>no600s to 900s</b>	38.39	32.51	37.81	37.43	36.15	36.46

**Table 8. Mean Group Vocal Periods (GVPs) for various Autogrouper configurations for the sample data from 2012-2016.**

	2012	2013	2014	2015	2016	CF (Means)
no100s / allhyd	0.99	1.00	0.99	1.00	1.00	1.00
no700s / allhyd	1.00	0.99	0.99	0.99	0.98	0.99
no900s / allhyd	1.00	0.99	0.99	0.99	0.99	0.99
no100s900s / allhyd	0.99	0.99	0.98	0.99	1.00	0.99
no100s600s700s / allhyd	0.98	0.99	0.98	0.98	0.98	0.98
no600s to 900s / allhyd	1.02	0.99	1.00	0.98	0.97	0.99

Table 9. Ratios of mean Group Vocal Periods (GVPs) in Table 8 for the various Autogrouper configurations to the Autogrouper run with all hydrophones. CF (the means of the ratios across years 2012 – 2016) indicates the correction factors derived for the GVPs.

#### 2.3.3.2.4 SOAR Correction Factors for the Number of Clicks per Group (Click Count)

Table 10 shows the mean number of clicks per group ('group click counts') for the various Autogrouper configurations. These data were used to calculate the ratios of the mean group click counts when hydrophones were missing to the mean group click counts when all hydrophones were present, and the means of these ratios were used as correction factors (Table 11). The group click counts, like the GVPs, do not vary much as a result of the different hydrophone configurations.

	2012	2013	2014	2015	2016	Mean
allhyd	1892.09	1685.73	2543.98	3312.12	2622.90	2411.36
no100s	1867.13	1714.23	2561.36	3309.15	2639.61	2418.30
no700s	1895.35	1660.48	2498.42	3213.05	2523.85	2358.23
no900s	1901.89	1638.85	2427.10	3212.93	2566.58	2349.47
no100s900s	1877.51	1661.16	2425.06	3193.89	2577.75	2347.07
no100s600s700s	1850.36	1685.96	2513.47	3164.28	2530.45	2348.90
no600s to 900s	1943.67	1637.11	2346.74	3074.68	2419.87	2284.42

Table 10. Mean group click count for various Autogrouper configurations for the sample data from 2012-2016.

	2012	2013	2014	2015	2016	CF (Means)
no100s / allhyd	0.99	1.02	1.01	1.00	1.01	1.00
no700s / allhyd	1.00	0.99	0.98	0.97	0.96	0.98
no900s / allhyd	1.01	0.97	0.95	0.97	0.98	0.98
no100s900s / allhyd	0.99	0.99	0.95	0.96	0.98	0.98
no100s600s700s / allhyd	0.98	1.00	0.99	0.96	0.96	0.98
no600s to 900s / allhyd	1.03	0.97	0.92	0.93	0.92	0.95

Table 11. Ratios of mean group click counts in Table 10 for the various Autogrouper configurations to the Autogrouper run with all hydrophones. CF (the means of the ratios across years 2012 – 2016) indicates the correction factors derived for the group click counts.

### 2.3.3.3 SOAR Legacy Hydrophones

#### 2.3.3.3.1 SOAR Data Samples

The CS-SVM ran on the legacy hydrophones for some archives in 2010-2012, and 2016-2017; therefore, a different sample dataset was used to determine the difference in number of *Zc* groups detected, the GVPs, and the number of clicks detected per *Zc* group, with or without using these hydrophones. Archive samples were selected that included both the newer hydrophones and the legacy hydrophones, and Autogrouper was run for all hydrophones. It was then run with the legacy hydrophones removed.

#### 2.3.3.3.2 SOAR Correction Factors for Number of *Zc* Groups (Dive Starts)

Table 12 shows the number of *Zc* groups detected for each year's samples with legacy hydrophones included and removed, along with the mean number of *Zc* groups detected from 2010 to 2017 ('means') and the total number of *Zc* groups detected from 2010 to 2017 ('sums'). The ratios of the number of *Zc* groups detected in Table 12 without using the Legacy hydrophones to the number detected when including Legacy hydrophones are indicated in Table 13, along with the ratio of the corresponding sums from Table 12. This ratio of the sums in Table 13 (total number of *Zc* groups detected from 2010 to 2017 without Legacy hydrophones to total number detected when including Legacy hydrophones) was used as the correction factor. About 16% fewer groups were detected when the legacy hydrophones were not used in the grouping process.

	2010	2011	2012	2016	2017	means	sums
<b>allhyds</b>	1387	3378	2151	972	8665	3310.6	16553
<b>noLegacy</b>	1220	2818	1912	972	7041	2792.6	13963

**Table 12.** Number of *Zc* groups detected for the samples in each year, for all hydrophones, and for Legacy hydrophones removed.

	2010	2011	2012	2016	2017	CF (sums)
<b>noLegacy / allhyds</b>	0.879596	0.834221	0.888889	1.000000	0.812579	0.843533

**Table 13.** Ratios of the number of *Zc* groups detected in Table 12 when Legacy hydrophones are removed to the number detected when Legacy hydrophones are included. CF (the ratio of the total number of groups detected without Legacy hydrophones to the total detected with Legacy hydrophones, for all sample years) indicates the correction factor derived for the number of *Zc* group dive starts.

#### 2.3.3.3.3 SOAR Correction Factors for the Group Vocal Periods (GVPs)

The mean GVPs for each year, both with and without the legacy hydrophones, are shown in Table 14, along with the means of the mean GVP from 2010 to 2017. The ratio of the mean GVPs in Table 14 without using the legacy hydrophones to the mean GVPs when including the Legacy hydrophones are shown in Table 15. The mean of the ratios in Table 15 was used as the correction factor. As with the case of missing hydrophone strings, the GVP is very consistent, whether or not the legacy hydrophones are included.

	2010	2011	2012	2016	2017	Means
<b>allhyd</b>	36.10	37.32	36.65	40.04	38.45	37.71
<b>nolegacy</b>	35.86	37.18	36.59	40.04	36.52	37.24

**Table 14.** *Zc* mean Group Vocal Periods (GVPs) for the samples in each year, for all hydrophones, and for Legacy hydrophones removed.

	2010	2011	2012	2016	2017	CF (Means)
<b>nolegacy / allhyds</b>	0.99	1.00	1.00	1.00	0.95	0.99

**Table 15.** Ratios of the *Zc* mean GVPs in Table 14 when Legacy hydrophones are removed to the GVPs when Legacy hydrophones are included. CF (the means of the ratios across all sample years) indicates the correction factor derived for the GVPs.

#### **2.3.3.3.4 SOAR Correction Factors for the Number of Clicks per Group (Group Click Counts)**

The mean numbers of clicks detected per *Zc* group with all hydrophones, and with legacy hydrophones removed, are shown in Table 16, along with the mean number of clicks per *Zc* group from 2010 to 2017. The ratios of the mean number of clicks detected per *Zc* group without Legacy hydrophones to the mean number detected using the Legacy hydrophones, from Table 16, are indicated in Table 17. The mean of the ratios from Table 17 was used as the correction factor. The mean number of clicks per group is consistent across hydrophone configurations.

	2010	2011	2012	2016	2017	Mean
<b>allhyd</b>	1882.85	2182.12	2007.28	3416.64	3102.95	2518.37
<b>nolegacy</b>	1908.2	2289.1	2038.41	3416.64	2558.35	2442.14

**Table 16.** *Zc* mean number of clicks detected per group for the samples in each year, for all hydrophones, and for Legacy hydrophones removed.

	2010	2011	2012	2016	2017	CF (Mean)
<b>nolegacy / allhyds</b>	1.01	1.05	1.02	1.00	0.82	0.98

**Table 17.** Ratios of the *Zc* mean number of clicks detected per group in Table 16 when Legacy phones are removed to the mean group click counts when Legacy phones are included. CF (the means of the ratios across the sample years) indicates the correction factor derived for the group click counts.

### 2.3.4 SOAR *Zc* Abundance

In 2010 Moretti, et al. described a passive acoustic method for determining Blainville's beaked whale density and abundance at the U.S. Navy's Atlantic Undersea Test and Evaluation Center (AUTEK) using a dive counting method. This method uses the start of a deep foraging dive, as indicated by the first detected click, as the cue for determining density and abundance. As *Md* and *Zc* have similar dive behavior, both consisting of small groups that conduct deep foraging dives synchronously, and producing echolocation clicks at depth [11], a modified version of this method has been applied to derive *Zc* abundance on the SOAR range.

The equation for animal abundance (*N*) presented by Moretti, et al. 2010 [13] was:

$$\text{Equation 1: } N = n_d s / r_d T$$

where:

$n_d$  = total number of dive starts

$s$  = average group size

$r_d$  = dive rate (dives/unit time)

$T$  = time period over which the measurement was made

For the Moretti et al. estimate, data were obtained over a relatively short time period, approximately six days around a multi-ship sonar exercise, and the data were manually reviewed. It was therefore assumed that the probability of detection was 1, and that there were no false positives. However, at SOAR there is a much higher density of marine mammals, and in particular delphinids, than at AUTEK. Also, this analysis is conducted over long time periods (years) with automated tools, as opposed to the manual analysis carried out at AUTEK; thus the abundance equation is modified to account for both the probability of detection (*PD*) and the proportion of false positives (*FP*).

The equation used for abundance in this analysis is:

$$\text{Equation 2: } N = n_d s (1 - c) / r_d T P_D$$

where:

$n_d$  = total number of dive starts

$s$  = average group size

$r_d$  = dive rate (dives/unit time)

$T$  = time period over which the measurement was made

$c$  = proportion of false positives

$P_D$  = probability of detection



### 3.0 SOAR Results

#### 3.1 SOAR Overview

SOAR archives were analyzed from August 2010 through September 2017. A total of 35,416.65 hours of data were processed, with the number of hours per year varying from a low of 2402 hours in 2010 to a high of 6297 hours in 2016 (Table 18).

Total Number of Hours of Effort							
2010	2011	2012	2013	2014	2015	2016	2017
2401.981	4983.139	3476.895	3565.143	5976.495	6009.888	6296.482	4205.000

Table 18. Total number of hours of effort per year in which data was recorded.

Figure 4 shows, for each year, the dive start GVPs plotted on the y-axis against the time of the year, with the effort start and stop periods, determined by finding gaps in effort greater than 24 hours, shown as green and red vertical lines, respectively.

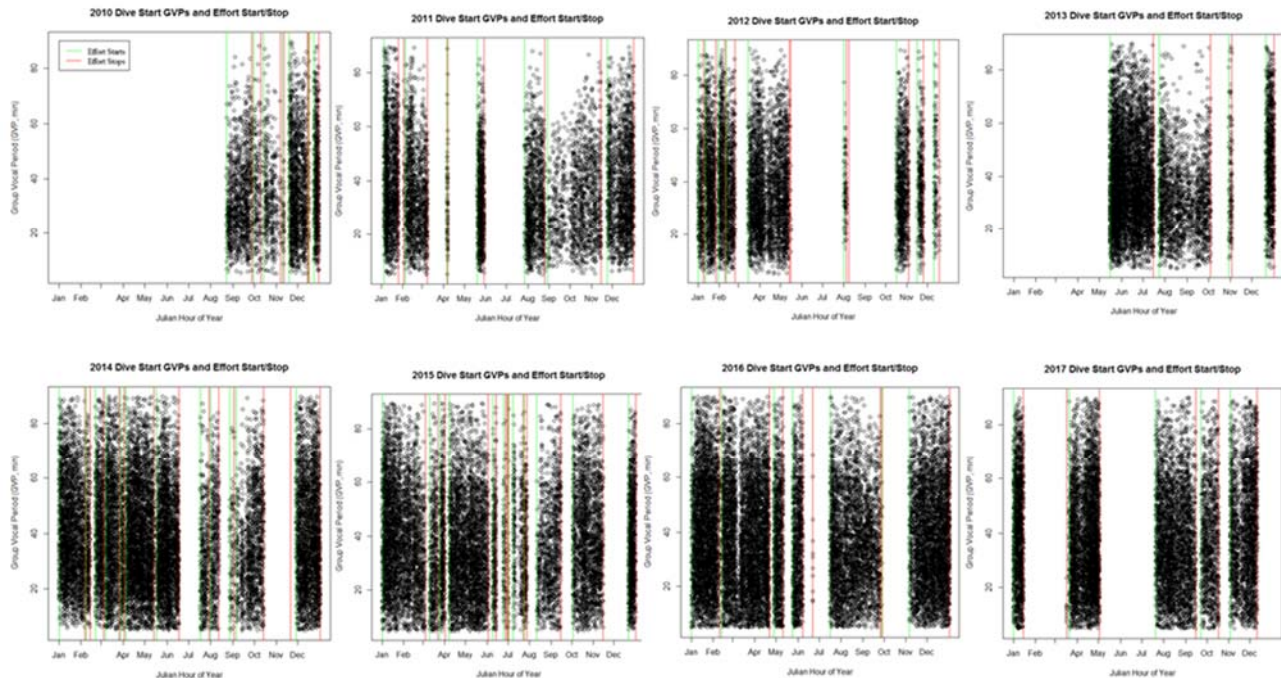


Figure 4. Dive start GVPs for each year along with effort start (green) and effort stop (red) times indicated with vertical lines. Effort start and stop times were calculated by finding gaps in effort greater than 24 hours.

The number of *Zc* dive starts per hour effort, total number of *Zc* clicks detected on range per hour effort, the *Zc* group vocal periods (GVPs), and *Zc* abundance were analyzed after cases of 'edge-only' groups were removed. 'Edge-only' *Zc* groups are those that are only detected on hydrophones on the edge of the range. They are removed on the assumption that these are groups that are located off the range.

### 3.2 SOAR Dive Starts per Hour Effort

The mean number of dive starts per hour effort for each month, averaged across the years 2010 through 2017 (Table 19), is shown in Figure 5, with the CVs used to calculate the confidence intervals in Table 20. It varies from a high of 3.52 dive starts per hour effort across the range in January to a low of 1.18 in September. The monthly mean number of dive starts per hour effort for each year is shown in Table 21 and Figure 6.

	Jan	Feb	Mar	Apr	May	Jun	Jul	Aug	Sep	Oct	Nov	Dec
<b>upper CI</b>	6.03	4.83	5.11	5.45	5.80	5.44	4.08	3.21	2.58	3.22	4.00	5.29
<b>mean # dive starts</b>	3.52	2.64	2.90	3.19	3.46	3.32	2.09	1.63	1.18	1.53	2.05	2.95
<b>lower CI</b>	1.01	0.45	0.69	0.94	1.12	1.20	0.11	0.06	-0.21	-0.15	0.10	0.62

Table 19. Mean monthly # dive starts per hour effort, averaged across 2010 to 2017

	Jan	Feb	Mar	Apr	May	Jun	Jul	Aug	Sep	Oct	Nov	Dec
<b>dive start CVs</b>	0.71	0.83	0.76	0.71	0.68	0.64	0.95	0.97	1.18	1.10	0.95	0.79

Table 20. Monthly CVs for the mean number of dive starts per hour effort, 2010 to 2017

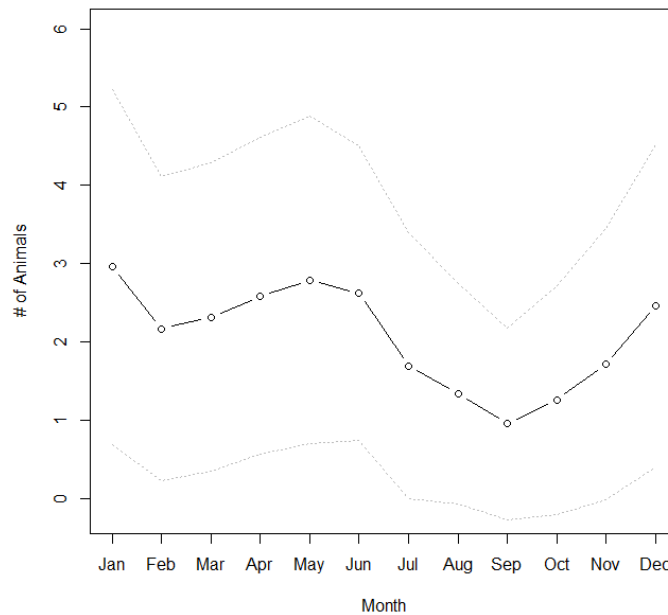
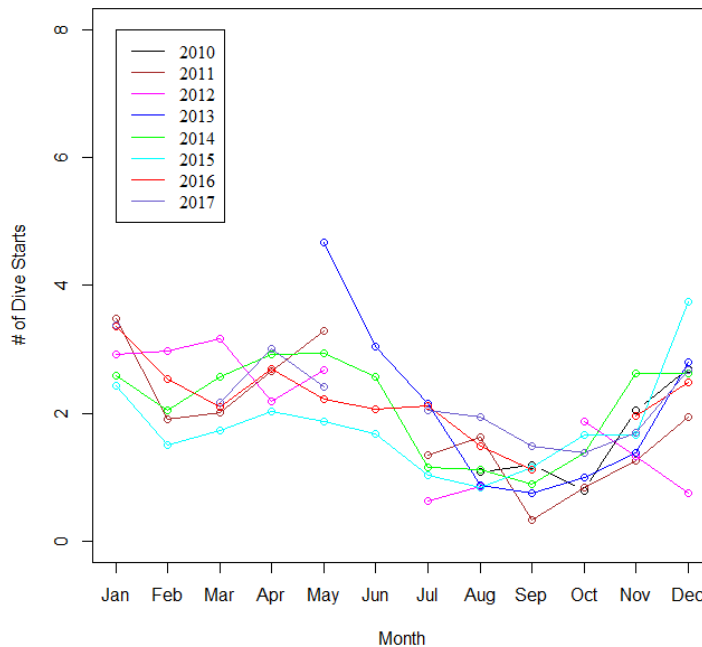


Figure 5. Mean monthly number of dive starts per hour effort, averaged across 2010 to 2017.

	Jan	Feb	Mar	Apr	May	Jun	Jul	Aug	Sep	Oct	Nov	Dec
<b>2010</b>	NA	NA	NA	NA	NA	NA	NA	1.08	1.19	0.80	2.05	2.69
<b>2011</b>	3.48	1.92	2.01	2.67	3.28	NA	1.35	1.63	0.33	0.84	1.26	1.94
<b>2012</b>	2.92	2.97	3.17	2.20	2.68	NA	0.64	0.86	NA	1.87	1.34	0.76
<b>2013</b>	NA	NA	NA	NA	4.66	3.05	2.16	0.88	0.75	1.01	1.38	2.80
<b>2014</b>	2.59	2.05	2.58	2.92	2.94	2.58	1.15	1.13	0.89	1.38	2.63	2.63
<b>2015</b>	2.44	1.50	1.74	2.04	1.88	1.69	1.03	0.84	1.15	1.66	1.67	3.75
<b>2016</b>	3.36	2.54	2.10	2.70	2.22	2.06	2.12	1.48	1.12	NA	1.95	2.49
<b>2017</b>	3.38	NA	2.16	3.00	2.42	NA	2.05	1.95	1.48	1.38	1.69	2.68

**Table 21: SOAR corrected monthly mean number of Zc group dive starts for 2010 to 2017**



**Figure 6. Mean monthly number of dive starts per hour effort for 2010 to 2017.**

In order to view the number of dive starts per hour on a 24-hour cycle the data was first corrected for the fact that there is varying effort over the years and a variation in the number of dive starts over each year. The mean number of dive starts per hour of the year across the years 2010 to 2017 was first plotted, and a fit to these data was found (**Error! Reference source not found.**). A 4<sup>th</sup> order fit to the mean values was then used to correct the dive start data by dividing each dive start data point by the corresponding fit value. The mean number of dive starts per hour was then generated for a 24-hour cycle.

The local San Clemente Island ‘day’/‘night’ periods were roughly considered from 7a-7p and 7p-7a, respectively. The sunrise and sunset times were averaged for the June and December solstices from 2010 through 2017, resulting in average sunrise and sunset times of approximately 0645 and 1854. Note also that the local time on San Clemente Island is 7 to 8 hours earlier than UTC, depending on Daylight Savings Time. The times associated with these data are in UTC. Note that

the apparent ‘banding’ in Figure 7 occurs either because there is only data available for one year during these time periods, or there is data for more than one year, but only one year has non-zero values. There is a drop in the number of dive starts per hour effort at night, with the lowest numbers at about midnight to 0100 local, and the peak at approximately 1300 to 1400 local time (**Error! Reference source not found.**). The lowest mean number of dive starts per hour is 1.78 at 0800 UTC, 2015, and the highest is 6.65 at 1900 UTC, 2017.

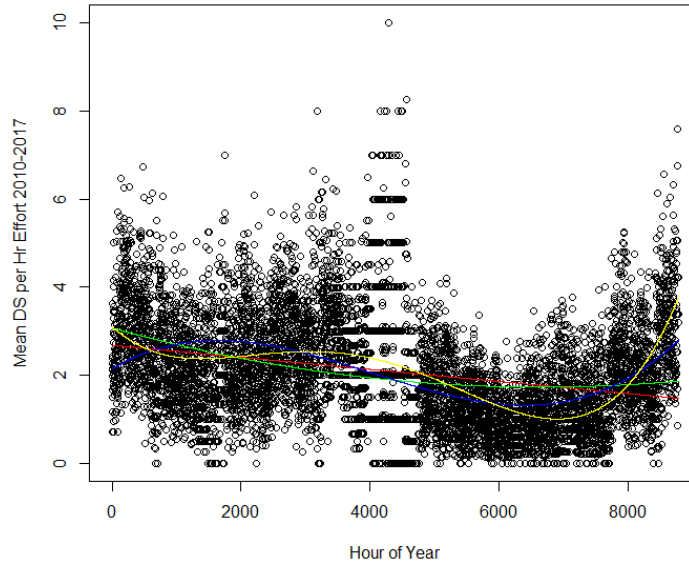


Figure 7. Number of Zc dive starts per hour averaged across 2010-2017 for every hour of the year, along with 1st to 4th order fits to the data. The 4th order fit used to correct the dive start data is shown in yellow.

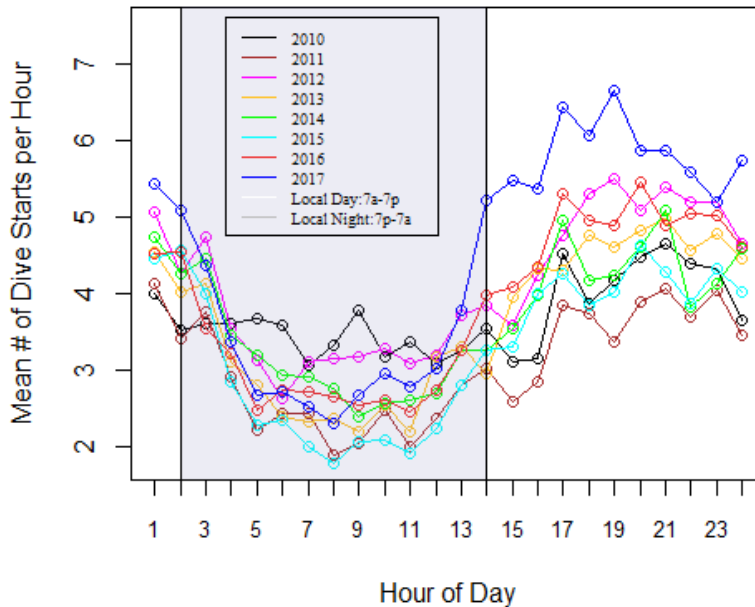


Figure 8. Mean number of Zc dive starts per hour on a 24-hour cycle. Note that the times are in UTC, and the gray shaded area indicates the approximate local night hours, if local day is considered 7a to 7p, and local night is considered 7p to 7a. There is a 7 or 8-hour difference between local time on San Clemente Island and UTC, depending on Daylight Savings Time.

### 3.3 SOAR Group Vocal Periods

The corrected mean monthly Group Vocal Periods (GVP) of the *Zc* dives were also calculated for 2010 through 2017, and averaged across 2010 to 2017 for each month (Table 22). The monthly mean across all years varies from a low of 36.00 min in August to a high of 42.53 min in January (Figure 9). The mean monthly vocal periods for each year, 2010 through 2017, are shown in Figure 10.

	Jan	Feb	Mar	Apr	May	Jun	Jul	Aug	Sep	Oct	Nov	Dec
<b>2010</b>	NA	NA	NA	NA	NA	NA	NA	29.57	35.27	35.52	37.16	38.06
<b>2011</b>	41.94	37.20	32.90	33.05	33.47	NA	31.18	32.90	32.28	34.52	39.28	38.89
<b>2012</b>	38.96	40.52	39.30	38.54	39.41	NA	40.35	39.14	NA	39.70	39.79	42.91
<b>2013</b>	NA	NA	NA	NA	40.14	41.02	39.53	33.75	33.15	38.80	38.70	48.04
<b>2014</b>	43.71	40.72	42.52	41.63	40.06	37.52	32.38	40.88	34.53	43.50	43.93	41.76
<b>2015</b>	44.30	39.25	36.13	38.11	37.28	36.26	40.90	35.41	43.40	43.38	42.09	40.14
<b>2016</b>	43.69	42.83	38.25	40.28	38.44	42.09	38.80	39.15	38.50	NA	41.82	41.30
<b>2017</b>	42.60	NA	38.98	39.58	39.15	NA	39.93	37.18	36.84	37.75	39.94	43.41
<b>monthly mean</b>	42.53	40.10	38.01	38.53	38.28	39.22	37.58	36.00	36.28	39.02	40.34	41.81

**Table 22. SOAR mean monthly corrected *Zc* group vocal periods (GVPs) for 2010 to 2017, and average across 2010-2017. NAs indicate missing data.**

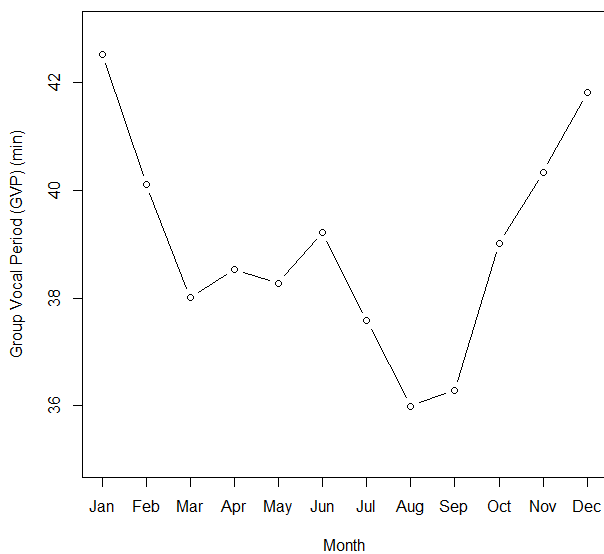


**Figure 9. SOAR corrected mean monthly *Zc* group vocal period (GVP), averaged across 2010-2017.**

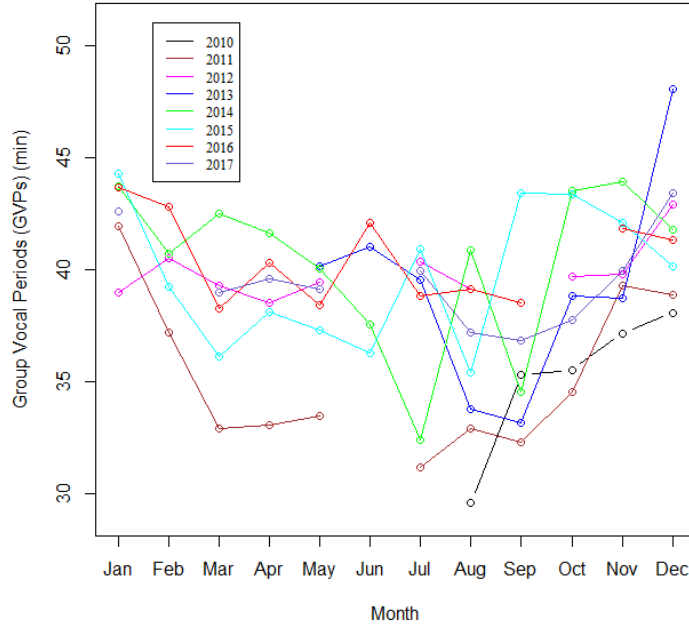


Figure 10. SOAR corrected mean monthly Zc group vocal period (GVP) for 2010 through 2017.

### 3.4 SOAR Zc Clicks per Hour

The corrected mean monthly Zc clicks detected per hour across the range for the years 2010 through 2017, and the average per month across 2010 to 2017, are shown in Table 23. The monthly mean varies from 1942 clicks in August to 3402 in January. The monthly mean across years is shown in Figure 11, and the monthly means for each year in Figure 12.

	Jan	Feb	Mar	Apr	May	Jun	Jul	Aug	Sep	Oct	Nov	Dec
<b>2010</b>	NA	NA	NA	NA	NA	NA	NA	951.51	1342.44	1484.70	2071.19	2415.06
<b>2011</b>	3137.64	2337.08	1729.77	1997.06	1561.30	NA	1426.86	1621.50	1018.63	1586.49	2281.74	2305.38
<b>2012</b>	2256.41	2407.99	2085.19	1873.58	1993.40	NA	2078.67	1615.34	NA	2233.39	1745.71	2056.23
<b>2013</b>	NA	NA	NA	NA	2103.03	2203.22	2106.64	1565.66	1841.90	2338.75	1961.49	3337.19
<b>2014</b>	2688.16	2331.29	3221.58	3343.09	2884.63	2466.94	2086.02	2655.37	2020.28	3391.75	4110.58	3760.43
<b>2015</b>	4437.71	3481.49	2945.53	2891.88	2583.12	3119.71	2775.24	1757.06	2910.99	3150.63	2652.97	2818.96
<b>2016</b>	3691.06	3344.40	2823.67	3269.91	3659.56	3936.67	2764.52	2588.75	2271.35	NA	2747.38	3346.72
<b>2017</b>	4201.87	NA	2784.96	3256.70	3243.71	NA	3029.88	2778.00	2799.15	2929.52	3182.80	3936.81
<b>monthly mean</b>	3402.14	2780.45	2598.45	2772.04	2575.54	2931.64	2323.98	1941.65	2029.25	2445.03	2594.23	2997.10

Table 23. SOAR mean monthly number of corrected Zc clicks per hour for 2010 to 2017, and average across 2010-2017. NAs indicate missing data.

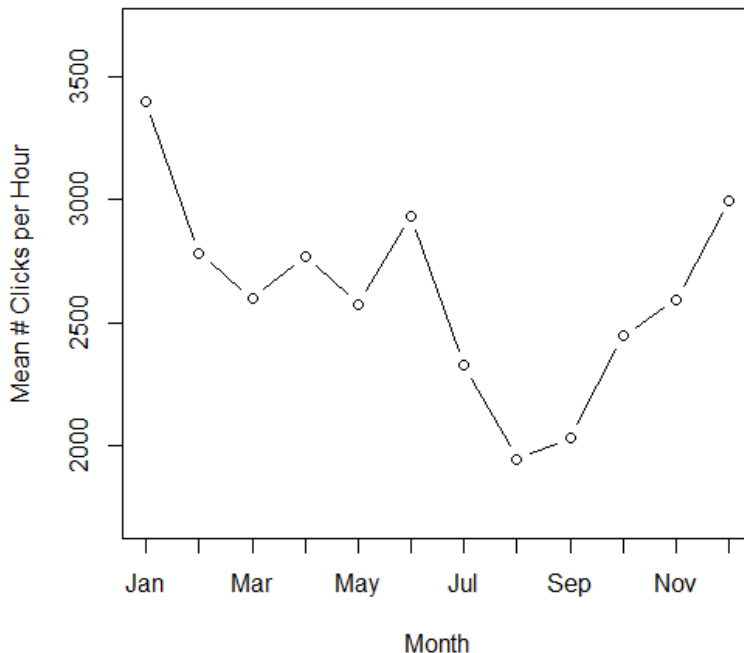


Figure 11. Corrected mean monthly number of Zc clicks detected per hour, averaged across 2010-2017.

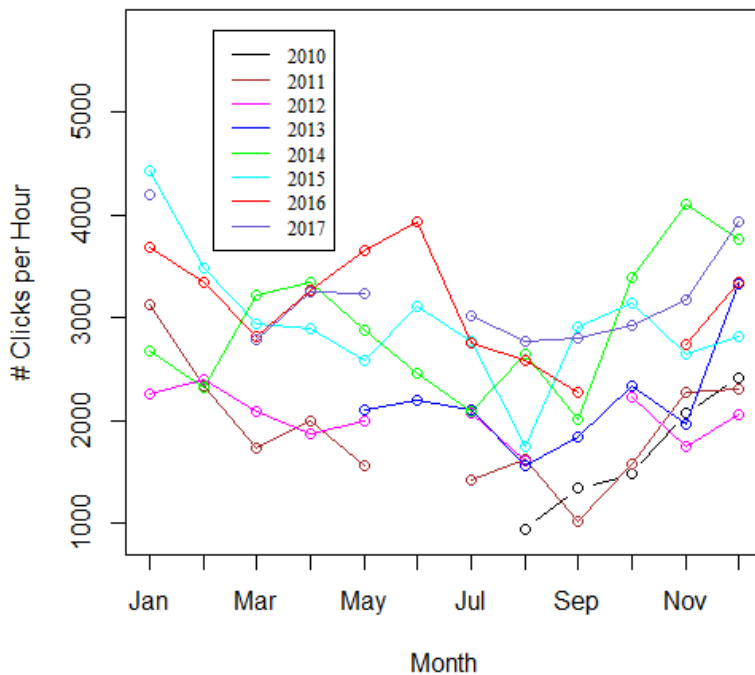
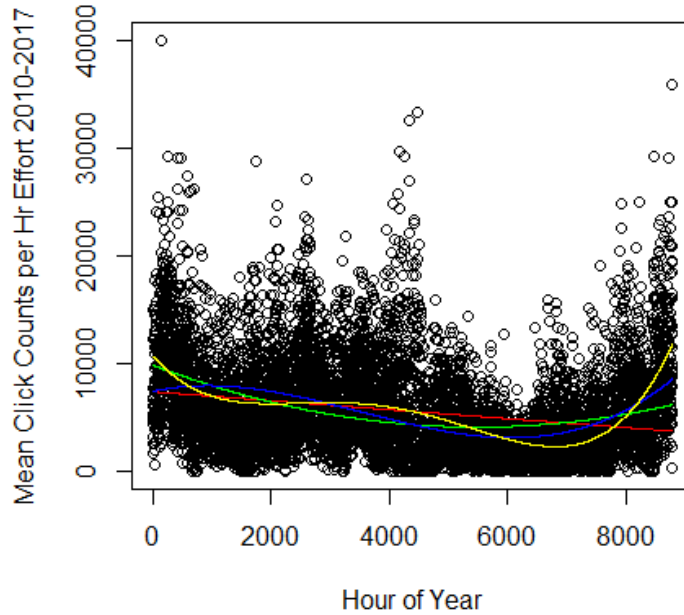


Figure 12. Correctly mean monthly number of Zc clicks detected per hour for the years 2010 through 2017.

The number of Zc clicks detected per hour across a 24-hour cycle was calculated after correcting the data with a 4<sup>th</sup> order fit to the mean number of clicks detected per hour from 2010 to 2017 (Figure 13), as in Section 3.2.



**Figure 13. Number of Zc clicks detected per hour across the range averaged across 2010-2017 for every hour of the year, along with 1st to 4th order fits to the data. The 4th order fit used to correct the dive start data is shown in yellow.**

As with the number of dive starts per hour effort, the number of clicks detected per hour effort drops at night, with the lowest numbers at about midnight to 0100 local, and the peak at approximately 1300 to 1400 local time (Figure 14). The lowest mean number of clicks detected across the range is 3,777.9 at 0900 UTC, 2011, and the highest is 35,170.7 at 1700 UTC, 2017.

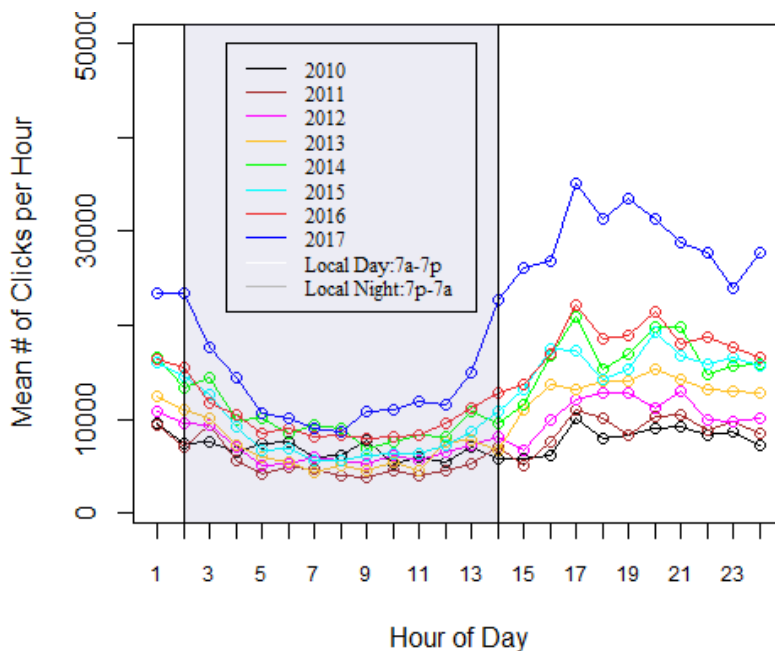


**Figure 14. Mean number of Zc clicks detected per hour on the range on a 24-hour cycle. Note that the times are in UTC, and the gray shaded area indicates the approximate local night hours, if local day is considered 7a to 7p, and local night is considered 7p to 7a. There is a 7 or 8-hour difference between local time on San Clemente Island and UTC, depending on Daylight Savings Time.**



### 3.5 SOAR Abundance

#### 3.5.1 SOAR Overview

Abundance was calculated at SOAR between 2010 and 2017 with all groups except those detected only on edge hydrophones, and the abundance equation 2 in section 1.3.4. The following values were used: average group size ( $s$ ) of 3.18 ( $CV = \pm 0.62$ ) (E. Falcone, pers. comm., December 06, 2017); dive rate ( $r_d$ ) of 0.3 ( $CV = \pm 0.17$ ), from Schorr et al. 2014 [7], proportion of false positives ( $c$ ) of 0.185 ( $CV = \pm 0.32$ ), probability of detection ( $P_D$ ) of 0.76 ( $CV = \pm 0.05$ ), and the total corrected number of dive starts ( $n_d$ ) and total hours of effort ( $T$ ) values as indicated in Table 24 and Table 25, respectively, for the monthly abundances. Abundance values were generated using numbers of dive starts corrected for both missing hydrophone strings and for the legacy hydrophones, as discussed in section 1.3.3. Confidence intervals, displayed in the following plots with dotted gray lines, were derived using the delta method as described in Moretti et al. (2010) [13, 14].

	Jan	Feb	Mar	Apr	May	Jun	Jul	Aug	Sep	Oct	Nov	Dec
<b>2010</b>	NA	NA	NA	NA	NA	NA	NA	258.7	843.8	579.7	1051.0	1352.1
<b>2011</b>	1838.7	1284.8	408.1	89.8	870.4	NA	186.9	1436.9	270.5	674.7	706.1	1551.1
<b>2012</b>	1879.4	1728.4	1593.0	1866.3	877.9	NA	17.6	73.1	NA	917.0	466.0	169.1
<b>2013</b>	NA	NA	NA	NA	2180.0	2648.0	1457.0	848.0	689.0	156.0	74.0	893.0
<b>2014</b>	2210.0	1186.0	1959.0	2415.0	2331.0	1316.0	447.6	541.9	801.3	566.0	154.0	2468.0
<b>2015</b>	2265.0	1312.0	1107.0	1558.0	1877.0	553.6	648.8	548.0	539.0	1599.9	772.1	1208.5
<b>2016</b>	3205.2	2137.9	2103.0	2091.0	1287.0	420.0	1063.0	1540.0	947.0	NA	1663.0	2433.9
<b>2017</b>	1338.7	NA	784.5	2377.9	91.1	NA	623.4	1589.2	873.1	593.8	1217.2	671.5

**Table 24. Total number of dive starts ( $n_d$ ) per month for 2010-2017 at SOAR. NAs indicate missing data.**

	Jan	Feb	Mar	Apr	May	Jun	Jul	Aug	Sep	Oct	Nov	Dec
<b>2010</b>	NA	NA	NA	NA	NA	NA	NA	210.9	629.3	623.2	473.3	465.3
<b>2011</b>	477.4	596.5	180.2	27.4	237.4	NA	122.5	629.4	720.0	744.0	504.5	743.9
<b>2012</b>	589.9	517.8	433.5	720.0	283.2	NA	23.8	67.3	NA	390.3	254.8	191.6
<b>2013</b>	NA	NA	NA	NA	391.6	720.0	553.4	743.8	720.0	125.1	46.1	265.1
<b>2014</b>	743.3	482.0	615.3	665.8	643.2	395.9	295.1	375.7	647.5	318.1	50.0	743.9
<b>2015</b>	743.9	671.8	485.5	568.8	744.0	223.5	456.8	488.4	338.3	702.6	342.9	243.5
<b>2016</b>	721.6	622.6	744.0	567.1	409.9	141.8	392.1	744.0	586.1	NA	626.6	740.7
<b>2017</b>	333.6	NA	271.5	699.0	36.0	NA	270.7	744.0	547.1	403.3	663.7	236.1

**Table 25. Total measurement time period per month, or total number of hours of effort per month ( $T$ ), for years 2010-2017. NAs indicate missing data.**

### 3.5.2 SOAR Monthly Abundance

The corrected mean monthly abundances at SOAR averaged from 2010 – 2017, along with CIs calculated using a CV of 0.71, are recorded in Table 26 and shown in Figure 15.

	Jan	Feb	Mar	Apr	May	Jun	Jul	Aug	Sep	Oct	Nov	Dec
<b>upper CI</b>	59.36	42.99	45.01	50.98	56.00	46.01	29.46	25.12	19.37	24.98	34.14	48.33
<b>mean abundance</b>	34.55	25.03	26.20	29.67	32.60	26.78	17.15	14.62	11.28	14.54	19.88	28.13
<b>lower CI</b>	9.75	7.06	7.39	8.37	9.19	7.56	4.84	4.12	3.18	4.10	5.61	7.94

**Table 26.** Mean monthly *Zc* abundances at SOAR averaged over 2010-2017, with CIs calculated using a CV = 0.71.

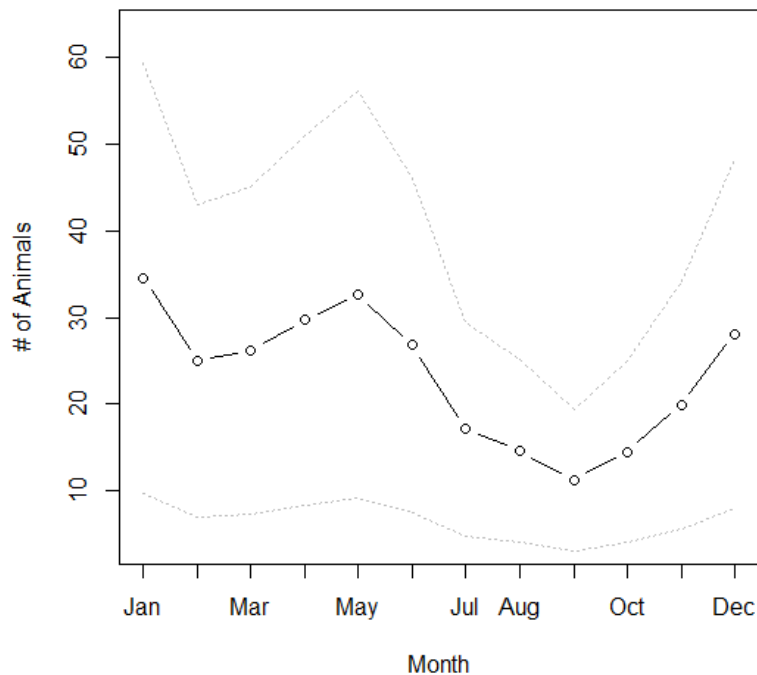


**Figure 15.** Corrected mean monthly *Zc* abundance at SOAR, averaged between 2010 and 2017.

The mean monthly *Zc* abundance shows a drop in September to 11.28 animals from a peak in January of 34.55 animals, followed closely in May with 32.60 animals, with a smaller dip in abundance in February to 25.03 animals. The drop in abundance in September is consistent with observations first reported by Simone Bauman-Pickering [personal communication 2017]. Table 27 has the corrected mean monthly abundance values for the years 2010 through 2017, and they are displayed in Figure 16.

	Jan	Feb	Mar	Apr	May	Jun	Jul	Aug	Sep	Oct	Nov	Dec
2010	NA	NA	NA	NA	NA	NA	NA	12.35	13.74	9.21	23.44	31.08
2011	40.00	21.89	22.81	31.50	37.49	NA	15.51	23.06	3.73	9.56	14.41	22.02
2012	33.42	33.89	36.10	24.91	30.47	NA	7.34	10.16	NA	21.29	15.17	8.65
2013	NA	NA	NA	NA	53.26	34.63	24.59	9.95	8.56	11.45	15.04	32.00
2014	29.43	23.35	29.44	33.30	33.48	29.20	13.22	12.94	10.16	15.66	30.47	29.82
2015	27.71	17.08	19.93	23.29	21.30	19.65	11.82	9.61	13.11	18.95	18.92	42.81
2016	38.22	28.93	23.85	30.75	25.27	23.66	24.15	16.82	12.82	NA	22.25	28.31
2017	38.55	NA	25.07	34.30	26.89	NA	23.42	22.08	16.83	15.67	19.32	30.39

Table 27. Mean monthly SOAR abundances for 2010 - 2017. NAs indicate periods without data.

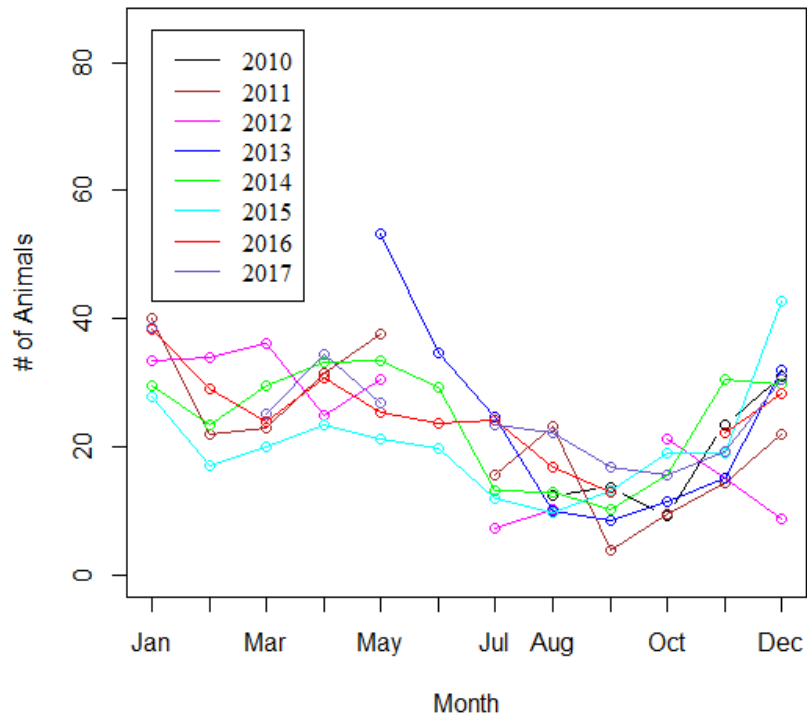


Figure 16. Corrected mean monthly Zc abundance for the years 2010-2017.

### 3.5.3 SOAR Yearly Abundance Trends

The yearly abundance means are affected by the time of the year in which data are collected, as there appears to be a seasonal change in abundance, and therefore to investigate any potential trends in abundance over the years, the corrected mean abundance was plotted for December, a month in which there was comparable effort for 2010 through 2017 (Figure 17).

The mean December SOAR abundance for 2010 to 2017, along with upper and lower CIs calculated with a CV of 0.71, are listed in Table 28.

	2010	2011	2012	2013	2014	2015	2016	2017
<b>upper CI</b>	53.39	37.84	14.85	54.97	51.22	73.55	48.63	52.21
<b>December mean abundance</b>	31.08	22.02	8.65	32.00	29.82	42.81	28.31	30.39
<b>lower CI</b>	8.77	6.21	2.44	9.03	8.41	12.08	7.99	8.57

Table 28. Mean December abundance from 2010 - 2016, with CIs calculated using a CV = 0.71.

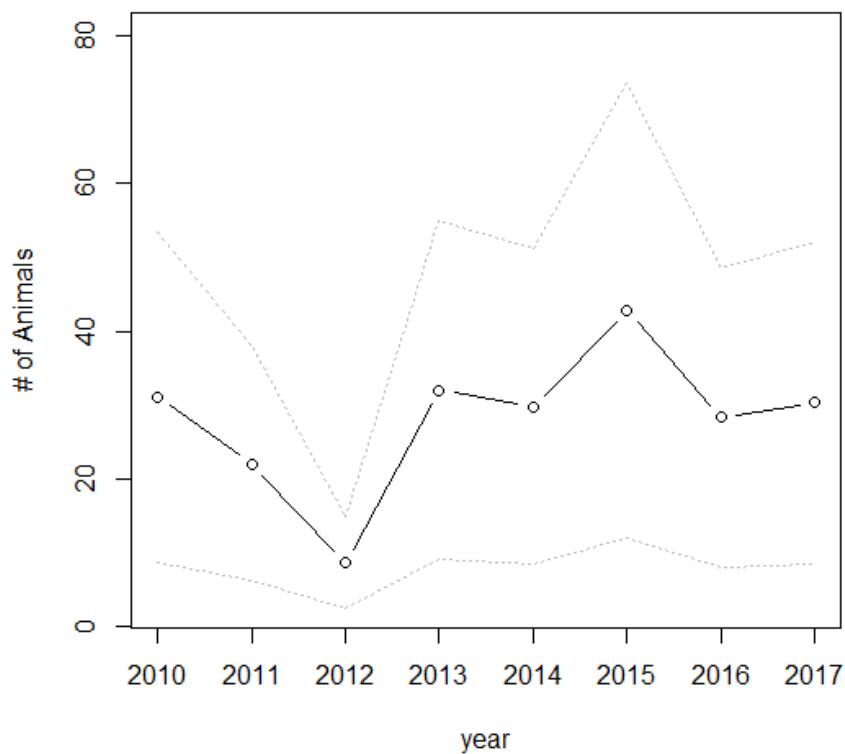
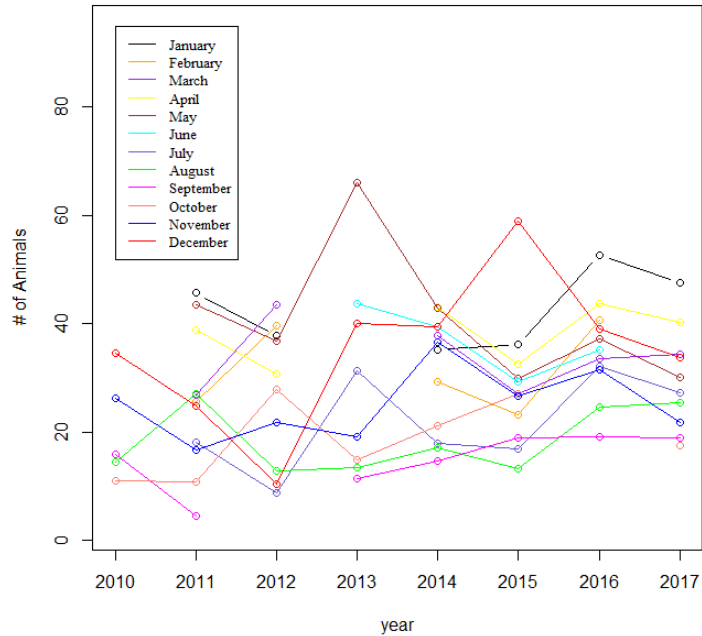


Figure 17. Corrected mean monthly *Zc* abundance for the month of December, 2010-2017.

The changes in corrected mean monthly abundance for each month, from 2010 to 2017, are shown Figure 18. It appears that the abundance from 2010 through 2017 is stable or has slightly increased.



**Figure 18. Corrected mean Zc abundances by month, from year 2010-2017.**

The uncertainty represented in the estimate via the delta method is calculated by combining uncertainty in each parameter estimate [13, 14]. However, each parameter is applied equally across years. Therefore, the trend reflected in the data will be preserved provided the base assumptions are correct.

The dive start method applied to the data assumes that the mean dive rate and group size are stable. Any changes will result in errors in the estimates.

### 3.5.4 SOAR Abundance on a 24-hour cycle

As for the number of dive starts and clicks detected per hour, the abundance can be viewed on a 24-hour cycle. To do this, the data was first corrected for the variance in effort and abundance over the years by dividing each data point by the corresponding 4<sup>th</sup>-order fit to the mean hourly abundance data over 2010 to 2017 (Figure 19).

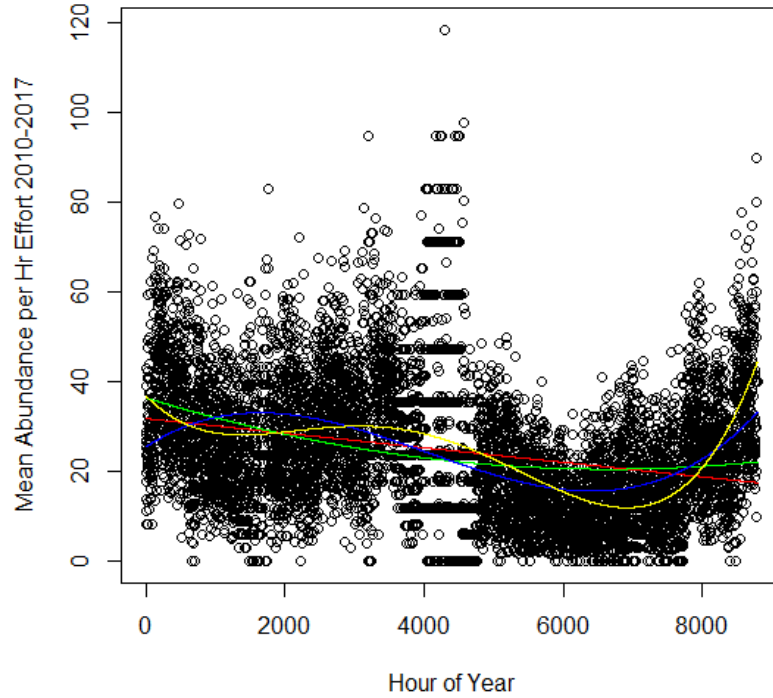


**Figure 19. Abundance per hour averaged across 2010-2017 for every hour of the year, along with 1st to 4th order fits to the data. The 4th order fit used to correct the dive start data is shown in yellow.**

The abundance per hour effort drops during the local night hours, with the lowest numbers at about midnight to 0100 local, and the peak at approximately 1300 to 1400 local time (Figure 20). The lowest mean abundance is 21.05 animals at 0800 UTC, 2015 and the highest is 78.9 at 1900 UTC, 2017.

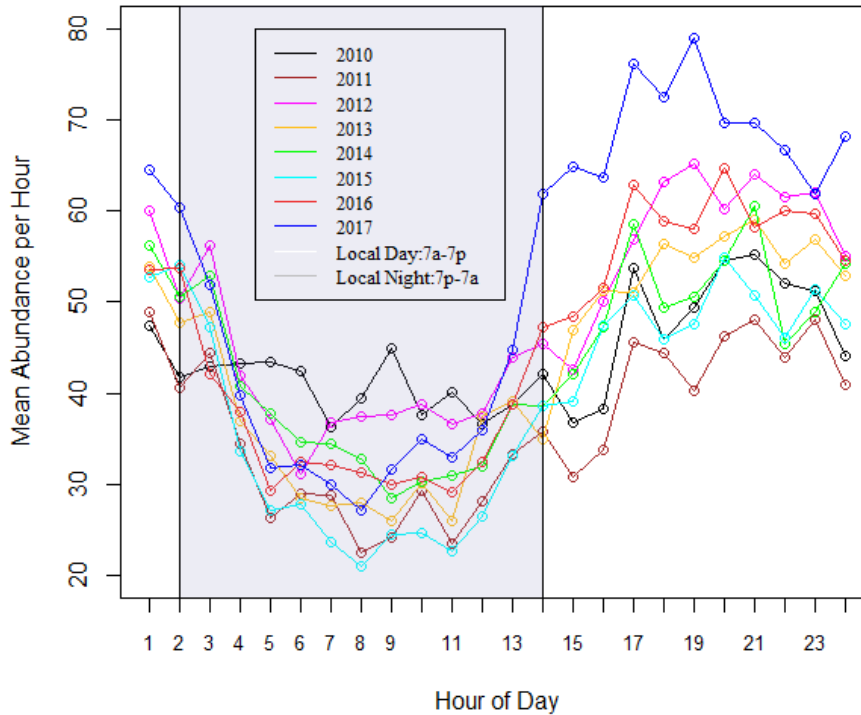


**Figure 20. Mean *Zc* abundance per hour on a 24-hour cycle. Note that the times are in UTC, and the gray shaded area indicates the approximate local night hours, if local day is considered 7a to 7p, and local night is considered 7p to 7a. There is a 7 or 8-hour difference between local time on San Clemente Island and UTC, depending on Daylight Savings Time.**

Note that as the apparent drop in *Zc* abundance, number of *Zc* dive starts per hour, and number of *Zc* clicks detected per hour during night-time hours does not appear to be consistent with satellite tag data on *Zc* at SOAR ([6], [7]), several factors should be examined that could explain the discrepancy. Following a discussion with T. Marques (pers. comm., 06/08/2018) of the University of St. Andrews, the following assumptions should be checked:

1. A constant probability of detection over the 24-hour cycle.
2. A constant probability of false alarms over the 24-hour cycle.
3. A constant dive rate over the 24-hour cycle.

In addition, current research by T. Marques on determining group size could be incorporated to see if group sizes vary over the 24-hour cycle.

J. Barlow of NOAA Southwest Fisheries Science Center also indicated that about 95% of dolphin detections occur on his group's sensors at night, and suggested that dolphin detections could be masking the *Zc* detections (pers. comm., 06/08/2018). Thus CS\_SVM 'Generalized Dolphin' detections should be examined on a 24-hour cycle to see if there is an increase in dolphin detections during night-time hours on SOAR.

## 4.0 Estimating the SOAR $Z_c$ risk function

### 4.1 SOAR Data

In 2016, a preliminary behavioral risk function for  $Z_c$  was completed using a methodology similar to that described for  $M_d$  by Moretti et al., 2014. This preliminary risk function estimated the probability of foraging dive disruption as a function of MFAS  $RL_{rms}$  exposure level, or the peak voltage reported by the FFT based sonar detector, and in 2017, work was completed to estimate the probability of foraging dive disruption as a function of MFAS sound pressure level (SPL) exposure level in dB re 1  $\mu$ Pa. Two datasets from the M3R system were used in this project that included data from 3-10 Feb 2012, 27 Jan-22 Mar 2014, 15 Apr-29 May 2015, and 6-8 Oct 2015.

The first dataset included in this project consisted of the time, location, frequency, and intensity of sonar pings at the SOAR range and was generated with an automated FFT-based sonar detection algorithm. Three separate sonar detector configurations were run that included 2500-4400 Hz, 3300-4900 Hz, and 6500-8500 Hz frequency bands. In each case, the detector was configured to output a detection report if the energy within the frequency band exceeded the background level by a user-specified multiplicative average for at least 10 of 93 consecutive time windows (106 ms of 1 s total). The sound pressure level (SPL) was then computed from the peak magnitude of the  $RL_{rms}$  for each detection report using the transfer function described in Section 5.0 of this report.

The second dataset for this project consisted of the time, location, and number of beaked whale vocalizations on the SOAR range during the study time periods. Generating this dataset used the same protocol as Moretti et al. (2014) and is briefly summarized here, but the reader is referred to that publication for details. The beaked whale detections were identified by first detecting individual beaked whale clicks in the archived hydrophone data, then applying an automated grouping algorithm, the “Autogrouper”, to cluster sets of clicks in group vocal periods (GVPs). The Autogrouper clustered individual clicks into click-trains for each hydrophone, then associated click-trains across hydrophones. It saved a list of records for further analysis that included the id of the hydrophone that detected each GVP, the number of detected clicks, and the start and end times for each group vocal period. In order to remove spurious detections, the final dataset used for this project included only GVPs with a minimum of 500 clicks.

### 4.2 SOAR Analysis

Using the sonar detection and beaked whale datasets, this project sought to identify how Navy sonar may impact beaked whale foraging behavior. Specifically, this project sought to estimate a risk function that would predict the probability of a GVP starting during a 30-minute time period given that active sonar operations were also ongoing during that same time window, because a GVP's start may be associated with the start of a foraging dive for  $Z_c$  (Johnson et al., 2006; Moretti et al., 2010). The project followed a similar analysis methodology to that presented in Moretti et al. (2014).

The preliminary analysis from 2016 estimated a risk function for  $Z_c$ , and ongoing analyses are in progress to refine the estimates for sonar exposure levels. For the preliminary analysis, the received SPL of sonar exposure for each GVP was estimated as the magnitude of the loudest sonar detection during that time period on the hydrophone that detected the most beaked whale clicks because it was assumed that the whales were in close proximity to this phone, and only sonar detections with



a peak magnitude exceeding 0.66 V were considered. Using the transfer function described in section 5 of this report, a peak magnitude of 0.66 V corresponds to 107 dB re 1  $\mu$ Pa SPL at the face of the hydrophone. Beaked whales likely decide whether to dive in the top 200 meters of the water column, but the hydrophones at SOAR are thousands of meters deep (Moretti et al. 2014). As a result, there is a substantial amount of attenuation and variability in SPL between the received SPL at the hydrophones and by the whales near the surface, and the threshold used in 2016 may exclude data that is necessary to accurately estimate the risk function. To better estimate the received SPL at the whale position, two analyses are ongoing.

The first ongoing analysis is the development of an automated algorithm to localize the source location of each sonar ping. Due to the intensity of the sonar pings and the oceanographic properties of SOAR, individual sonar pings may be detected by many or all of the hydrophones at SOAR. Detections may include both direct-path and multi-path propagation channels, and some of the detections may be noise rather than sonar pings. As a result, the algorithm must correctly associate detections on multiple hydrophones as originating from the same ping while discarding spurious detections, then localize the source time and position for each ping. To complete the first objective, associating the detections across hydrophones, a set of algorithms that seek to minimize a tunable objective function have been implemented. The objective function in use seeks to minimize the residual squared error between the estimated and observed arrival time for each detection that is associated with a sonar ping, and penalizes this arrival time by the number of detections that are not associated with a sonar ping. Let  $t_i$  be the time that detection  $i$  is detected, let  $t_0$  be the estimated time of emission for the sonar ping,  $r_i$  be the predicted distance from the emission source to the hydrophone that detected the ping, and  $n$  be the number of detections that are not associated with a sonar ping. Then Eq. 3 gives the value of the objective function to be minimized, where 1500 m/s is the nominal speed of sound in seawater and  $\lambda$  is a user-specified tuning parameter.

$$\text{Equation 3: } \sum_i \left( t_i - t_0 - \frac{r_i}{1500} \right)^2 - \lambda n$$

The sonar detection dataset contains tens of millions of detections, so brute force optimization of the objective function is not computationally tractable. Instead, a greedy optimization heuristic that processes short time windows in chronological order and attempts to minimize the objective function within that time window without revisiting prior windows is applied. As part of the optimization process, it is necessary to estimate the source position of each sonar ping to obtain  $t_0$  and  $r_i$ . The source time and position is estimated to minimize the squared residual error between the predicted and observed detection times given the hydrophone positions and a nominal sound speed of 1500 m/s. The optimization procedure has been used to process the full sonar detection dataset, and the identification of a suitable validation dataset is ongoing. The vehicle positions computed from this procedure can then be used with propagation modeling to estimate the received SPL at each whale's position.

The second ongoing approach to better estimate the received SPL at the whale positions relies on the procedure used by Moretti et al. (2014). Under this approach, the source position of assets on the SOAR range will be identified from GPS logs, and propagation modeling will be used to estimate the received SPL at each whale's position.

Based on the analysis reported here, the presence of active sonar operations at SOAR decreases the probability of observing a GVP start during the same time window. Assuming that the GVP starts are associated with the initiation of foraging dives by beaked whale groups, it may be inferred from this result that sonar operations influence beaked whale behavior. Once the results of the sonar localization and propagation modeling analyses are available and have been used to estimate a risk function, the relationship between the sonar exposure intensity and beaked whale behavior will be better known. The automated sonar localization algorithm will also offer the potential to process and include an increased quantity of data, which will result in a more precise estimate for the risk function.

## **5.0 SOAR and BSURE hydrophone calibration**

### **5.1 SOAR and BSURE Overview**

The hydrophones at SOAR and PMRF are being used to passive acoustically monitor marine mammals in-situ (Jarvis et al. 2014). Although the M3R system has been effectively used to study the response of marine mammals to naval training in its current form, its capabilities would be greatly enhanced if the sound pressure level (SPL) at the face of each hydrophone could be readily computed from the detections on the M3R system.

The M3R system may be configured for either real-time or retrospective processing, and many of the algorithms follow the same processing pipeline regardless of configuration. The sound pressure level (SPL) at the face of each hydrophone is converted to an analog electrical signal that is processed in both analog and digital form by the Ocean Sensor System (OSS) and Shore Electronics System (SES) before reaching the input to the M3R system (Figure 21). Within the M3R system, the signal is sampled at 96 kHz, then passed through a 2048 point Fast Fourier Transform (FFT) with a rectangular window and 50% overlap (Jarvis et al. 2014). The result of this processing is a frequency domain signal,  $\mathbf{X}$ , with 46.875 Hz frequency resolution and 10.67 ms time resolution. Although some of the detection algorithms further process this signal as part of their operation, ultimately it is the magnitude of the frequency domain signal within a specific time and frequency bin that is reported as the intensity of the detected sound.

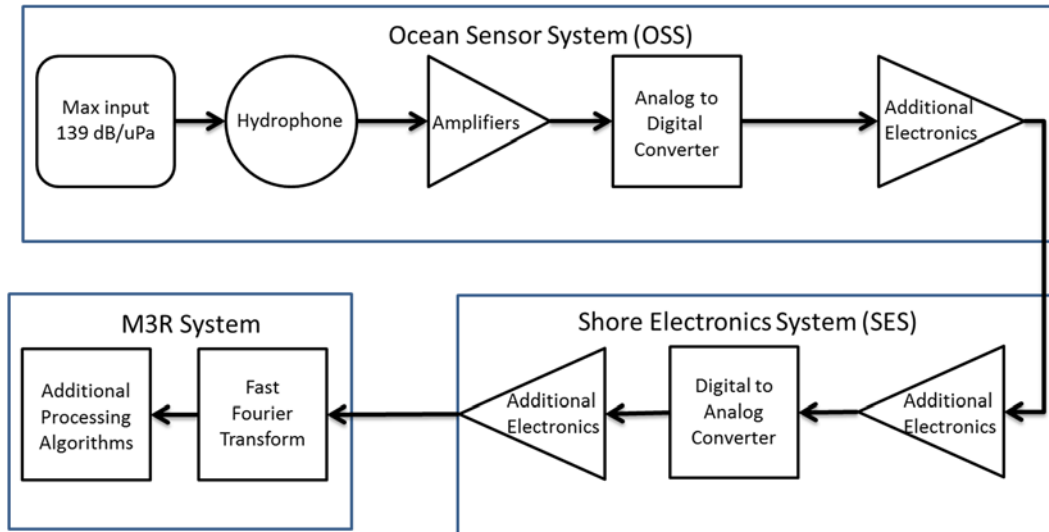


**Figure 21. Data acquisition system block diagram**

The M3R system has been successfully applied to a variety of questions regarding marine mammal ecology. One such study was Moretti et al. (2014), which used the M3R system to estimate a risk function for Blainville's beaked whale behavioral responses to naval sonar exposure at the Atlantic Undersea Test and Evaluation Center (AUTECE). In this study, the researchers used the M3R system to identify the start times of *Md* foraging dives and also to identify time periods when naval sonar was active on range. They then estimated the exposure level of each whale to sonar using a two-step process: (1) identify ship positions from a database of GPS ship tracks and (2) estimate exposure levels using a propagation model and the known ship positions. Finally, the authors conclude with a risk function that gives the probability of behavioral response across a range of sonar exposure intensities. This risk function provides the Navy and others with additional information to assist in compliance with environmental regulations.

This project involved the estimation of a transfer function to compute the SPL at the face of each hydrophone from the frequency domain signal,  $\mathbf{X}$ , in the M3R system at SOAR, which may assist in studies similar to the Moretti et al. (2014) one discussed above. The transfer function would permit automated estimation of the sonar intensity directly from the M3R archives and may eliminate the necessity of analyzing ship track databases and applying propagation modeling. The automated process would also facilitate affordable analysis of larger datasets, which would improve the accuracy of the estimated risk function. More generally, we expect that this transfer function will have applications for a variety of studies that use the M3R system.

## 5.2 SOAR and BSURE Transfer function estimation

A two-step process was applied to estimate and validate the transfer function. First, a transfer function from the analog signal intensity at the output of the SES,  $V_{SES}$ , to the SPL at the face of the hydrophone was computed based on published system specifications for the OSS and SES. Second, a transfer function from the M3R output,  $\mathbf{X}$ , to  $V_{SES}$ , was computed from measurements obtained at NUWC DIVNPT. Together, these two functions are considered the transfer function from the M3R output to the SPL.

The maximum signal analysis system gain block diagram for the Southern California Anti-Submarine Range (SOAR) system specifies the maximum input SPL, maximum output levels of the analog to digital converter (ADC) and digital to analog converter (DAC), and gains throughout the OSS and SES systems. Figure 16 depicts a simplified version of this diagram with the technical specifications removed, and this project assumes that the SOAR system is equivalent to the SOAR system.

The system diagram indicates the amplitude of the maximum input signal to the hydrophone and maximum output signal from the SES. Using this information alone, it is possible to solve Eq. 4 for  $\alpha$  and obtain a transfer function from the SES output to the SPL. Eq. 4 assumes that  $V_{SES}$  is expressed in root mean square volts ( $V_{rms}$ ).

$$\text{Equation 4: } \text{SPL} = 20 \times \log_{10}(V_{SES}) + \alpha$$

The calculation of the transfer function from the M3R system output to the SES output was based upon data from a replica M3R system at NUWCDIVNPT (Figure 22). The signal generator was configured to output a fixed amplitude sine wave with frequencies of 1523 Hz for the first test and 15023 Hz for the second test. These frequencies were chosen to lie near the center of a 46.875 Hz frequency bin in  $X$ . This signal was attenuated at a range of values from 0 dB to -90 dB, then passed into an oscilloscope and the M3R system. At each frequency and attenuation value, the peak to peak voltage was measured on the oscilloscope and the magnitude of the reports from the M3R system was noted.

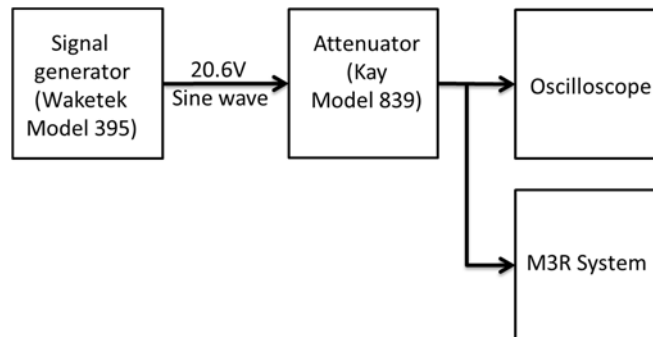


**Figure 22. Test system block diagram**

The attenuated signal amplitude,  $S$ , was computed as a function of each attenuation level,  $A$ , and the maximum signal using Eq. 5. The correlation coefficient for the relationship between the measured and calculated attenuated signal levels was 0.999.

$$\text{Equation 5: } S = 10^{A/20}$$

The M3R processing system passes the analog signal through an analog-to-digital converter, applies a Hanning window, then computes the FFT. The relationship between the input  $S$  and output  $X$  for this process may be expressed as a gain after converting the input and output to dB, and the gain may be calculated by Eq. 6.

$$\text{Equation 6: } \text{Gain} = 20 \log_{10}(X/S)$$

The ratio of the inter-quartile range to the median value for the estimated gain, calculated across all of the lab measurements, was 0.027, which indicates that the estimated median is likely highly accurate. The signal **S** in our replica configuration is equivalent to  $V_{SES}$  in the operational system at SOAR, so it was possible to combine these relationships to compute a full transfer function from the M3R output to the SPL at the face of the hydrophone. Interested parties should contact NUWCDIVNPT regarding the technical data and specifications.

Using this information and the system specifications documents, it is possible to compute transfer functions for subcomponents of this system.

### **5.3 SOAR and BSURE Validation using real-world data**

The final transfer function from the face of the hydrophone to the level reported in an M3R detection report was validated using real-world data from MK 30 ASW acoustic target tracks. For multiple close approaches to a hydrophone, the receive level at the face of the hydrophone was estimated using Eq. 7:

$$\text{Equation 7: } RL = SL - 20\log R - \text{absorp} * R - \text{BWL}$$

where:

RL = Receive Level at the face of the hydrophone

SL = 193 dB = MK 30 Source Level

R = Range from the MK 30 to the hydrophone

absorp = 0.001541 = absorption coefficient (in dB/m) for 12.931 kHz, 1000 m depth, 5 deg C

BWL = Energy loss because the MK 30 signal is not a pure sine wave within a single frequency bin

For the validation, five minutes of data centered on the closest point of approach were used for multiple passes.

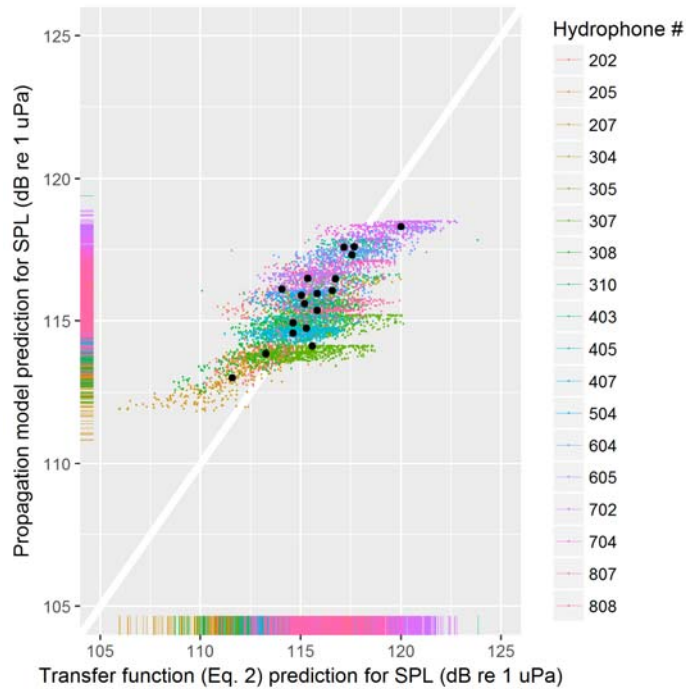


**Figure 23.** The relationship between the predicted sound pressure level (SPL) from the MK 30 positions and propagation model are plotted as a function of the predictions from the laboratory validation. The colored dots depict the data with color indicating the hydrophone that detected the MK 30 ping. The black dots indicate the median value for each hydrophone and the white diagonal line in the background is a 1-1 line. The rug plots along the horizontal and vertical axis depict the projection of the data point onto that axis.

For each detection in the MK 30 dataset, the SPL was estimated using the peak magnitude ( $SPL_{PM}$ ) and the transfer function ( $SPL_{TF}$ ) as derived above. Comparison of  $SPL_{PM}$  and  $SPL_{TF}$  indicates that they are similar and appear to be a 1-1 match (Figure 23). The substantial variability in the observed values may be explained by the directivity pattern of the hydrophone sensitivity and variability in the environment. The calibration reports for the SOAR/BSURE refurbishment indicate that at 12931 Hz, the individual transducer sensitivities are -1 dB to -4 dB relative to their nominal value for a signal that is directly overhead. The sensitivities smoothly increase to 0 dB to -1 dB relative to their nominal value at approximately 60 degrees offset from directly overhead. The variability of the observed values among measurements on each hydrophone and between the hydrophones is likely due to variability in the angle of the acoustic ray relative to the hydrophone and variability in the acoustic environment.

The techniques applied to develop this function could be applied to estimate transfer functions for other components of the SOAR system as well as additional sets of hydrophones including the BARSTUR hydrophones. The data and techniques presented in this report will assist in future studies that use the M3R system or subcomponents of it.

## 6.0 PMRF Study Site

### 6.1 PMRF Overview

The Pacific Missile Range Facility is located off the northwest coast of Kauai, HI. The range consists of the three distinct areas, known as the Barking Sands Tactical Underwater Tracking Range (BARSTUR), the BARSTUR Expansion (BSURE) and the Shallow Water Tracking Range (SWTR). For this analysis, hydrophones for BARSTUR at depths of approximately 1-2 km and BSURE with hydrophones at depths of 2-4 km were used in this analysis (Figure 24).

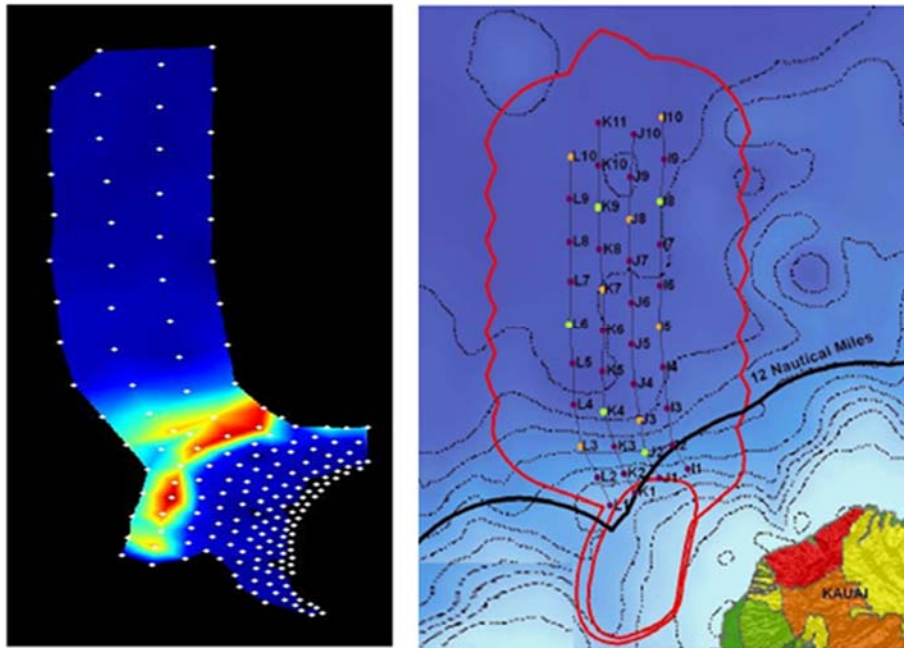


Figure 24. An outline of the PMRF range is on the right. The PMRF range boundaries are indicated by the outer red line. The BARSTUR range area is indicated by the inner red line. The left plot shows the distribution of beaked whale click detections for the time period 11-Jun-2012 through 02-Aug-2012. The dots represent the range hydrophones including those in SWTR.

The BSURE hydrophones are identical to those described in section 2.1 for SOAR. BARSTUR consists of 42 hydrophones with a bandwidth of approximately 8-45 kHz with six broadband hydrophones that cover a bandwidth of approximately 20 Hz to 45 kHz.

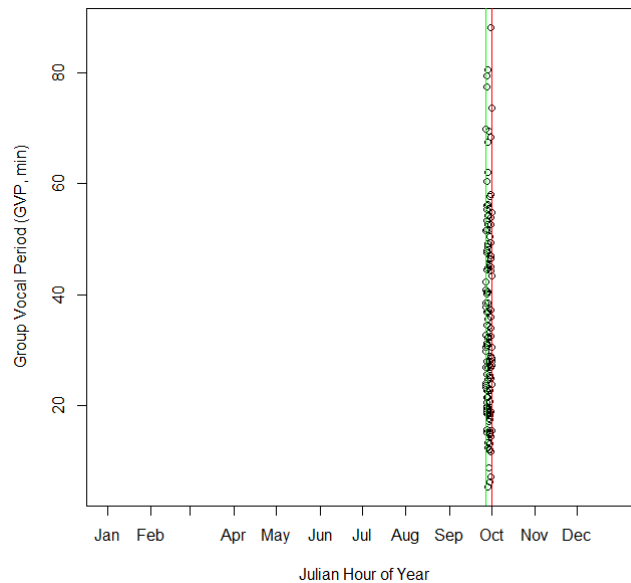
### 6.2 PMRF Abundance

#### 6.2.1 PMRF Data Summary

PMRF archives were analyzed from 2015 through 2017. Through 2016 data were only collected during tests at PMRF when M3R personnel were on range to start the M3R archiver, typically in advance of an SCC event. Data were collected during the event and after as long as the system remained running. Typically, however, the system was rebooted within days of the completion of the event for a number of reasons, including classified operations, power outages, etc. As the M3R archiver did not automatically restart during these reboots, only a small amount of archive

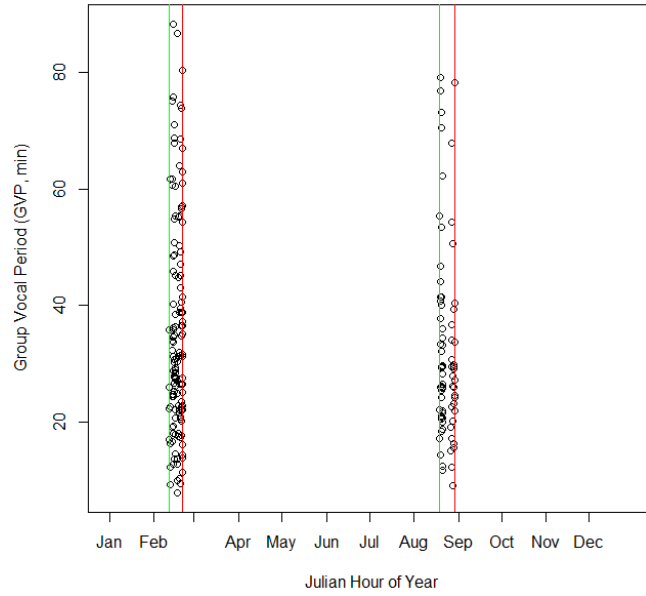
data was collected in 2015 and 2016. In 2017 an operational system was configured to run in parallel to the R&D system and on-site technicians were charged with its maintenance, to ensure continuous archiving of the M3R data. The data presented here include the first extended archive which runs from February until August of 2017. In August, 2017 the archive disk was recovered from PMRF and a new archive was initiated.

Figure 25, Figure 26, and Figure 27 show, for years 2015 through 2017 respectively, the periods for which M3R archives are available. Specifically, the plots show the PMRF *Md* dive start group vocal periods (GVPs) plotted on the y-axis against the time of the year. The vertical green lines indicate the starts of periods of effort, and vertical red lines indicate the stops. The gaps in effort indicated (time between stop and start) are at least 24 hours in length.



**Figure 25. PMRF *Md* dive start GVPs for 2015 along with effort start (green) and effort stop (red) times indicated with vertical lines. Effort start and stop times were calculated by finding gaps in effort greater than 24 hours.**





**Figure 26. PMRF *Md* dive start GVPs for 2016 along with effort start (green) and effort stop (red) times indicated with vertical lines. Effort start and stop times were calculated by finding gaps in effort greater than 24 hours.**

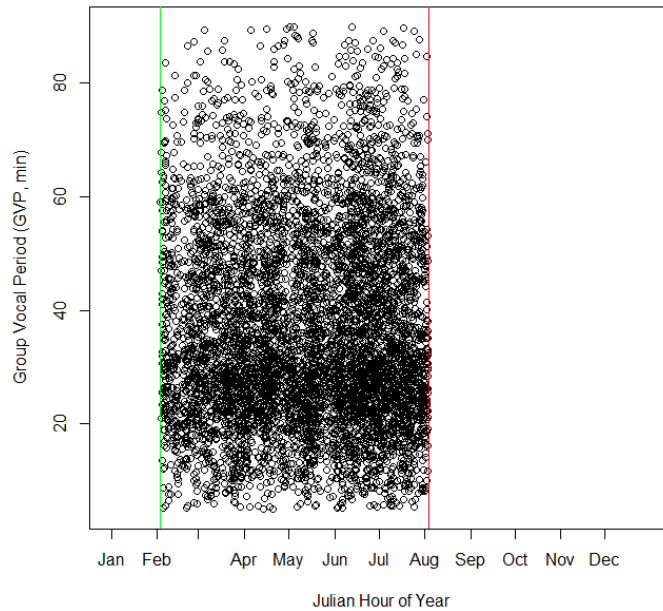


**Figure 27. PMRF *Md* dive start GVPs for 2017 along with effort start (green) and effort stop (red) times indicated with vertical lines. Effort start and stop times were calculated by finding gaps in effort greater than 24 hours.**

Correction factors for the probability of detection and false alarm rate at PMRF for the CS-SVM detector are being measured. For the initial results presented here correction factors calculated for *Md* at AUTECH were used. While the absolute abundance numbers are likely to change, the trends presented in the plots below will remain unchanged. Results presented in the past (2011-2014) were calculated using an FFT-based detector, whereas the 2015-2017 results were derived from CS-SVM detections. Once correction factors are applied, the data will be combined to present a continuous estimate from 2011 to the present.

### 6.2.2 PMRF Abundance

*Md* abundance was calculated at PMRF between 2015 and 2017 using all groups detected, and the abundance equation 2 in section 2.3.4. The following values were used: average group size (*s*) of 3.6 [10]; dive rate (*r<sub>d</sub>*) of 0.42 (average of mean day/night, [11]), proportion of false positives (*c*) of 0.17, probability of detection (*P<sub>D</sub>*) of 0.86.

The mean monthly *Md* abundance for which we have data peaks in June at 16.56 animals, with the lowest numbers in August, 2016 (2.57 animals) and February, 2016 (5.07 animals). The mean monthly abundances from 2015 through 2017 are shown in Table 29.

	Jan	Feb	Mar	Apr	May	Jun	Jul	Aug	Sep	Oct	Nov	Dec
<b>2015</b>	NA	NA	NA	NA	NA	NA	NA	NA	11.38	6.66	NA	NA
<b>2016</b>	NA	5.07	NA	NA	NA	NA	NA	2.57	NA	NA	NA	NA
<b>2017</b>	NA	7.96	11.24	12.02	12.12	16.56	14.2	13.08	NA	NA	NA	NA

**Table 29.** Mean monthly *Md* abundances for PMRF, 2015-2017. NAs indicate missing data.

The mean PMRF *Md* abundance per year is shown in Figure 28, and the monthly *Md* abundances for each year are shown in Figure 29.

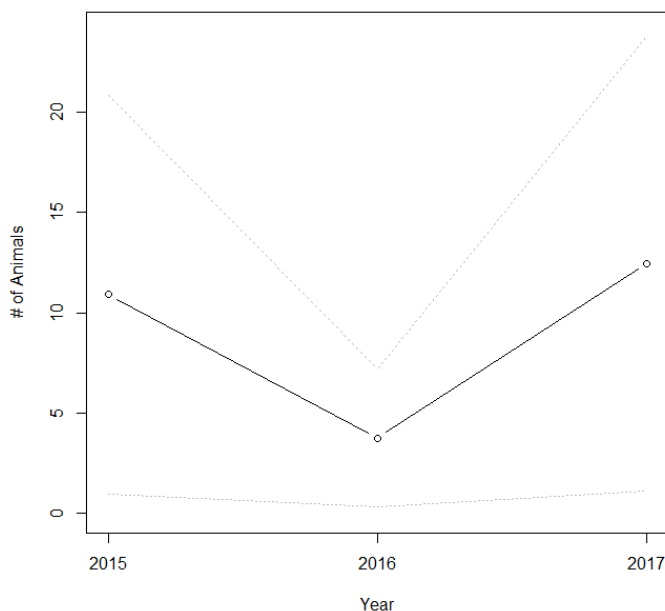


**Figure 28.** Mean PMRF *Md* abundance per year from 2015-2017.

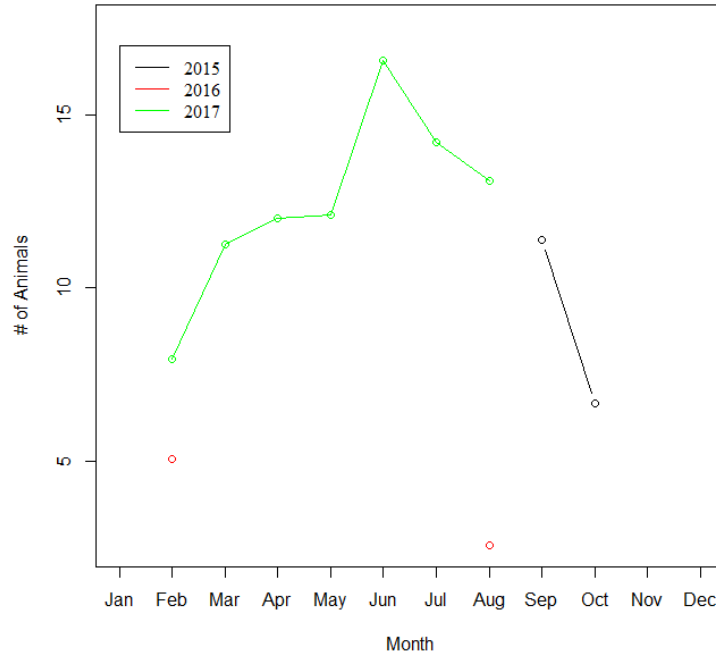


**Figure 29. Mean monthly *Md* abundance for years 2015-2017.**

The sonar detector is being run in real-time and ping detection reports are being integrated into the M3R archives. This will allow definitive long-term monitoring for sonar activity. These sonar data can then be combined with cetacean detection data to inform the long-term study of the effect of sonar on cetaceans.

Figure 30 presents the daily estimate of *Md* abundance for February, 2017, along with the output from the sonar detector. The data suggest an apparent reduction in abundance coincident with a multi-ship MFAS event between 14-18 February.

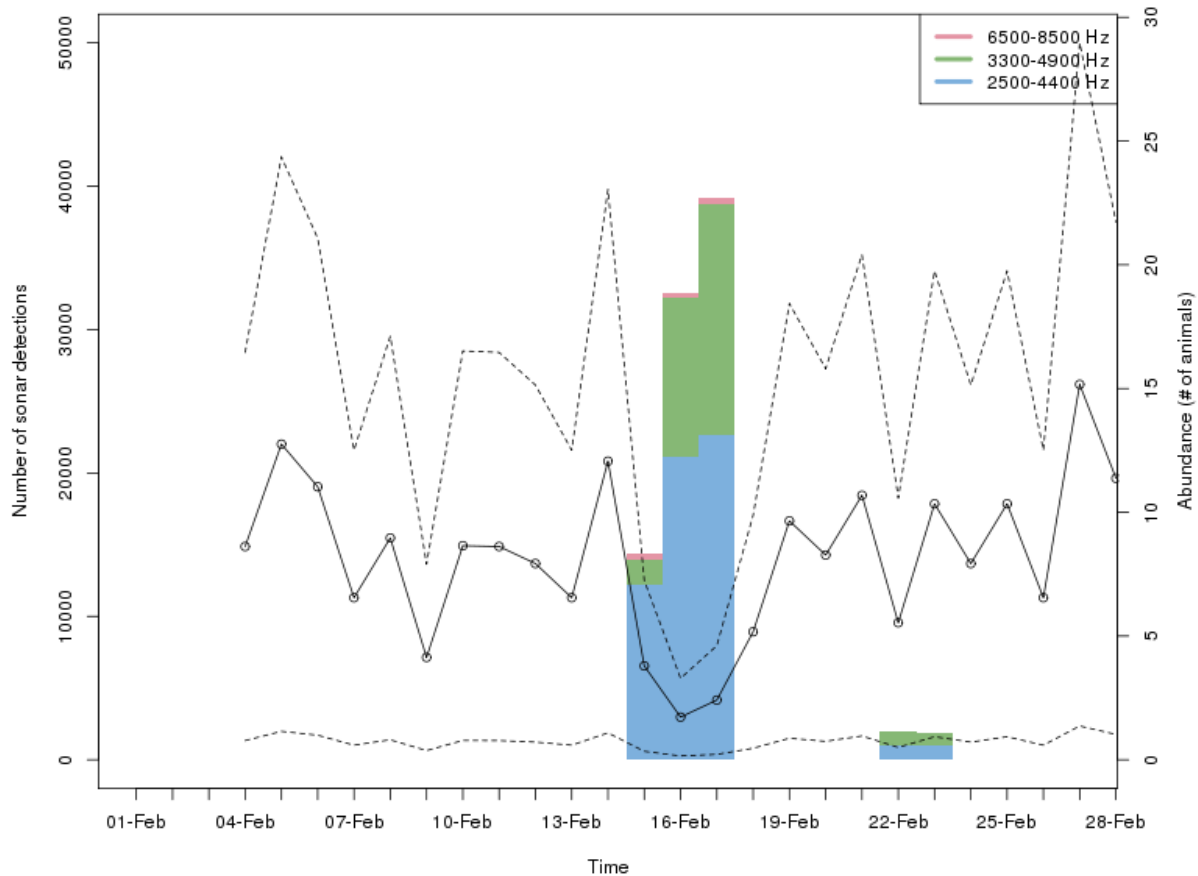


**Figure 30.** Daily *Md* abundance for the month of February 2017 in black (dotted lines = 95% CI). Detections from the sonar detector for all range hydrophone are presented by the colored bars.

### 6.3 PMRF *Md* behavioral risk function

A behavioral dose-response function for Blainville's beaked whales at the Pacific Missile Range Facility (PMRF), using passive acoustic data collected at the range hydrophones, is being derived. The initial analysis uses data collected by SPAWAR around multi-ship sonar operations at PMRF, and will be expanded with extended M3R archived data that include unit level tests and dipping helicopter deployed MFAS. Recordings were processed to derive timing of the start of the acoustic part of beaked whale group dives ("group dive starts") and the hydrophone estimated to be closest to the dive location. Statistical methods are being developed to determine if there is a change in the number or location of group dive starts associated with Navy activity as a function of MFAS exposure level, source distance and exposure duration.

Such analysis must account for two factors before an effect analysis can be performed. Firstly, hydrophone spacing is non-uniform – where hydrophones are closer together they in some sense "compete" to be group dive start centers, and so one would expect lower counts where hydrophones are denser. Therefore the analysis must account for the amount of area around each hydrophone where groups diving could be counted as coming from. Secondly, group dive starts

are not distributed uniformly in space or time even under baseline conditions, and this must also be accounted for.

For the former issue (non-uniform hydrophone spacing) a tessellation-based partition of the area around the PMRF hydrophones (Figure 31) was derived, assuming an effective detection radius of 6.5 km outside the hydrophone array.

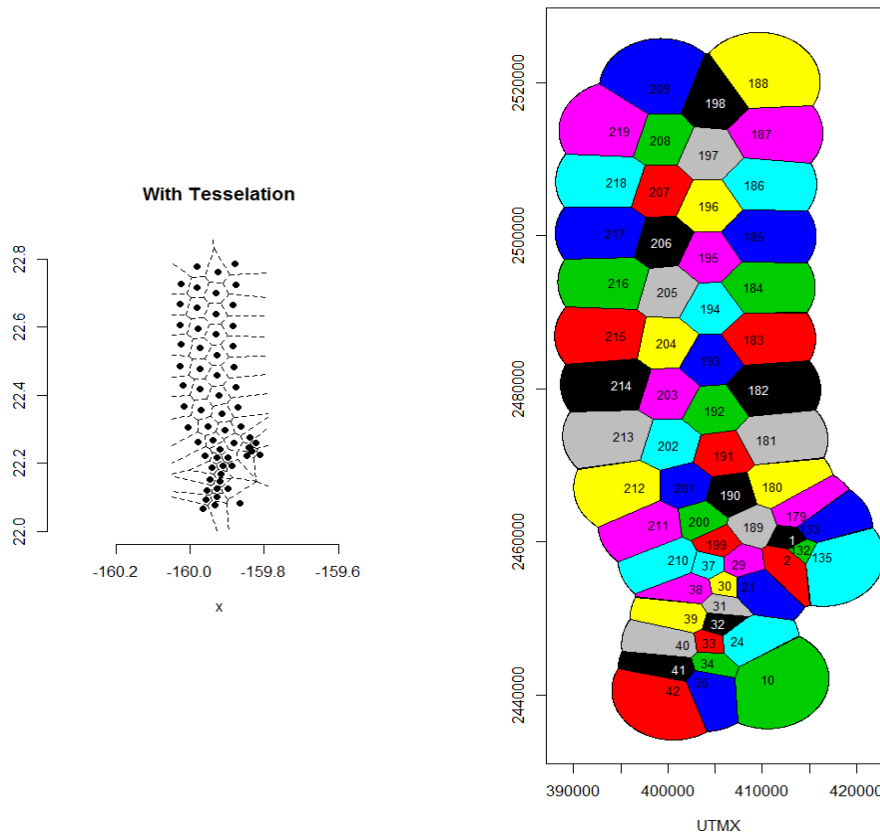


**Figure 31. Locations (jittered) of the 62 hydrophones includes in the SPAWAR dataset, with simple tessellation tiles on the left and improved tiles (assuming a 6.5km effective detection radius) on the right.**

To address the second issue, of non-uniform distribution of dive starts in space and time, group dive starts are being modelled using a Generalized Additive Modelling (GAM) framework to account for spatial and temporal variation, and residual temporal correlation in dive starts as necessary. Test data come from a multi-ship training exercise at PMRF in August 2013. Modelling has also involved the potential inclusion of additional explanatory variables such as depth (Figure 32). We are currently working on fitting variables related to Navy activity such as ship type, estimated received level, etc. Assuming these models produce a good fit to the data, they will yield the first dose-response estimates.

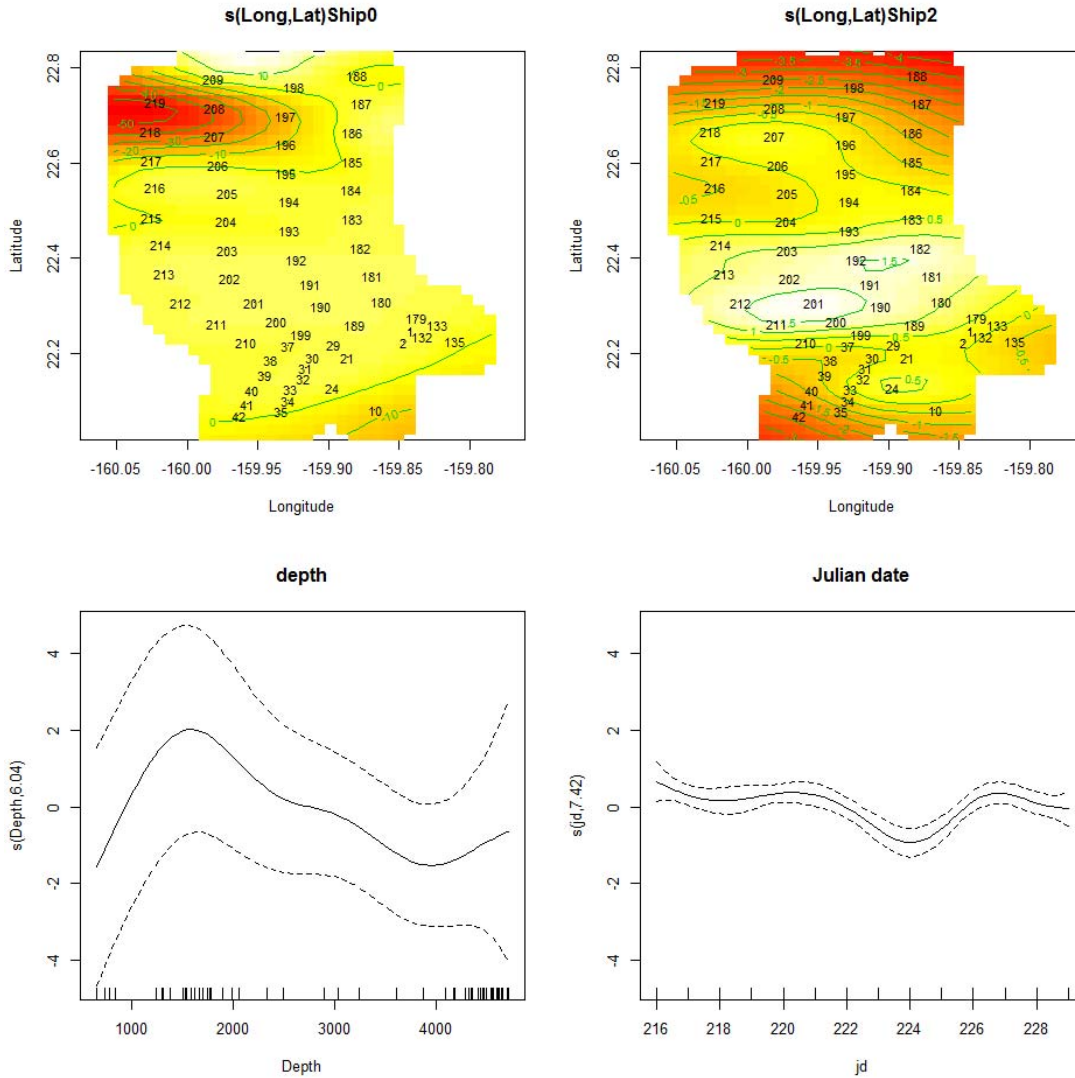


**Figure 32. Partial fit plots for smooths from binomial GAM, on the scale of the logistic link function. The 2-dimensional spatial smooth term  $s(\text{Longitude}, \text{Latitude})$  is illustrated in the heat plot showing a 2-D spatial smooth with hydrophone locations. Contour lines in heat plots represent surfaces at  $\pm 0.5, 1, 1.5$  standard errors. Vertical lines in the smooth for covariates depth and Julian date indicate locations of observations.**

## 7.0 Works Cited

- [1] E. L. Hazen, D. P. Nowacek, L. St. Laurent, P. N. Halpin and D. J. Moretti, *The Relationship among Oceanography, Prey Fields, and Beaked Whale Foraging Habitat in the Tongue of the Ocean*, vol. 6(4), 2011.
- [2] K. Benoit-Bird, M. Moline and B. Southall, "Predator-guided sampling reveals biotic structure in the bathypelagic," *Proceedings of the Royal Society B: Biological Sciences*, vol. 283, no. 1825, February 2016.
- [3] G. S. Schorr, E. A. Falcone, B. K. Rone and E. L. Keene, "Distribution and demographics of Cuvier's beaked whales in the Southern California Bight," Marine Ecology and Telemetry Research, NUWC Contract N66604-14-C-0145 Final Report, Seabeck, WA, 2018.
- [4] R. W. Baird, D. L. Webster, S. M. Jarvis, K. A. Wood, C. J. Cornforth, S. D. Mahaffy, K. K. Martien, K. M. Roberston, D. B. Anderson and D. J. Moretti, "Odontocete Studies on the Pacific Missile Range Facility in August 2017: Satellite-Tagging, Photo-Identification, and Passive Acoustic Monitoring," Cascadia Research Collective, NAFAC Pacific Report: Contract N62470-15-D-8006, Olympia, WA, 2018.
- [5] E. Falcone, G. Schorr, A. Douglas, J. Calambokidis, E. Henderson, M. McKenna, J. Hildebrand and D. Moretti, "Sighting characteristics and photo-identification of Cuvier's beaked whales (*Ziphius cavirostris*) near San Clemente Island, California: a key area for beaked whales and the military?," *Marine Biology*, vol. 156, pp. 2631-2640, 2009.
- [6] E. A. Falcone, G. S. Schorr, S. DeRuiter, D. L. DeRuiter, A. N. Zerbini, R. D. Andrews, R. P. Morrissey and D. J. Moretti, "Diving behaviour of Cuvier's beaked whales exposed to two types of military sonar," *Royal Society Open Science*, 2017.
- [7] G. S. Schorr, E. A. Falcone, D. J. Moretti and R. D. Andrews, "First Long-Term Behavioral Records from Cuvier's Beaked Whales (*Ziphius cavirostris*) Reveal Record-Breaking Dives," *PLoS ONE*, vol. 9, no. 3, March 2014.
- [8] S. M. Jarvis, R. P. Morrissey, D. J. Moretti and J. A. Shaffer, "Detection, Localization, and Monitoring of Marine Mammals in Open Ocean Environments using Fields of Spaced Bottom Mounted Hydrophones," *Marine Technology Society Journal*, vol. 48, no. 1, pp. 5-20, Feb. 2014.
- [9] S. Jarvis, *A Novel Method for Multi-Class Classification Using Support Vector Machines*, 2012.
- [10] M. Team, Marine Mammal Effects from T & E on Ocean Ranges (METEOR) Final Report, Test Resource Management Center, Advanced Instrumentation System Technology, Dr. George Shoemaker (george.shoemaker@navy.mil), Executing Agent, 2014.
- [11] P. L. Tyack, M. Johnson, N. Aquilar Soto, A. Sturlese and P. Madsen, *Extreme Diving of Beaked Whales*, vol. 209, 2006, pp. 4238-4253.
- [12] W. X. Zimmer, M. P. Johnson, P. T. Madsen and P. L. Tyack, "Echolocation clicks of free-ranging Cuvier's beaked whales (*Ziphius cavirostris*)," *Journal of the Acoustical Society of America*, vol. 117(6), pp. 3919-3927, 2005.
- [13] D. Moretti, T. Marques, L. Thomas, N. DiMarzio, A. Dilley, R. Morrissey, E. McCarthy, J. Ward and S. Jarvis, "A dive counting density estimation method for Blainville's beaked whale (*Mesoplodon densirostris*) using a bottom-mounted hydrophone field as applied to a Mid-Frequency Active (MFA) sonar operation," *J. Applied Acoustics*, vol. 71(11), pp. 1036-1042, 2010.
- [14] G. A. F. Seber, *The Estimation of Animal Abundance*, 2nd ed., London: Griffen, 1982.

*This page intentionally left blank.*



## Appendix A: SOAR Click Train Processor (CTP) file list

Table 30 contains a list of all the SOAR click train processor (CTP) files from 2010 to 2017, which were used to generate Zc groups.

The samples used for calculating correction factors for the 'missing hydrophone strings' case are highlighted in yellow in Table 30, and those used for the 'legacy hydrophone' case are highlighted in pink.

CTP filename	Year	UTC Start Time	UTC Stop Time	CS-SVM: newer Hyds NOT Detected	CS-SVM on Legacy Hyds?
spc_08222010_2130pdt_1-103	2010	235:04:30:15.578048	236:03:49:32.160922	100's	yes
spc_082310_2125pdt_1-1284	2010	236:04:24:44.017389	250:16:03:44.385787	100's	yes
spc_09072010_1204pdt_2-1489	2010	250:19:22:57.323181	266:16:01:13.181995	100's	yes
spc_09232010_0904pdt_2-49	2010	266:16:17:58.201671	267:01:58:08.761928	100's	yes
spc_09242010_1148pdt_1-22	2010	267:19:04:22.611408	267:23:26:06.626187	100's	yes
spc_09252010_0828pdt_1-277	2010	268:15:27:18.997476	271:00:00:40.083523	100's	yes
spc_09292010_0820pdt_1-42	2010	272:15:20:33.828750	272:23:15:37.623506	100's	yes
spc_09292010_1650pdt_1-12	2010	272:23:52:05.863845	273:02:15:49.791995	100's	yes
spc_09302010_0811pdt_1-2	2010	273:15:08:31.798232	273:15:23:46.113957	100's	yes
spc_09302010_0835pdt_1-152	2010	273:15:34:30.891334	274:22:35:23.608460	100's	yes
spc_10012010_1550pdt_1-42	2010	274:22:51:00.306996	275:07:15:06.007250	100's	yes
spc_10022010_1905pdt_1-652	2010	276:02:12:46.851126	281:16:07:18.888197	100's	yes
spc_10082010_13220pdt_1-183	2010	281:20:24:17.493510	283:15:58:29.966006	100's	no
spc_10132010_1300pdt_1-982	2010	286:20:04:01.532266	296:11:08:49.698217	100's	no
spc_10232010_1640pdt_1-9	2010	296:23:42:58.664980	297:02:48:05.744725	100's	no
spc_10232010_1640pdt_14-99	2010	297:03:56:44.131572	298:02:44:54.044084	100's	no
spc_10232010_1640pdt_130-489	2010	298:10:05:09.556736	302:14:27:56.220842	100's	no
spc_10292010_0730_mod_pdt_1-30	2010	302:14:30:39.035321	303:00:10:39.814107	100's	no
spc_10292010_0730pdt_31-924	2010	303:00:13:44.089532	310:17:43:20.361676	100's	no
spc_11092010_0810pdt_1-31	2010	313:16:15:40.865605	313:21:41:56.820989	100's	yes
spc_11092010_1340pdt_1-214	2010	313:21:44:17.014260	315:15:41:56.288828	100's	yes
spc_11182010_1547pdt_1-856	2010	322:23:48:00.825657	335:09:22:10.899431	100's, 900's	yes
spc_12012010_1154pdt_1-161	2010	335:19:54:39.548647	336:22:01:16.021122	100's, 900's	yes
spc_12022010_1404pdt_1-468	2010	336:22:04:42.229692	340:16:06:51.624995	100's, 900's	yes
spc_12062010_1427pdt_1-447	2010	340:22:27:32.260943	344:20:09:38.273660	100's, 900's	yes
spc_12102010_1335pdt_1-431	2010	344:21:35:44.226966	348:05:52:26.103023	100's, 900's	yes
spc_12152010_1614pdt_1-42	2010	350:00:13:10.632007	350:10:18:08.330326	100's, 900's	yes
spc_12232010_1122pdt_1-762	2010	357:19:22:59.833653	364:07:04:29.341024	100's, 900's	yes
2011_01_04SOAR_spcarch_1-15	2011	004:18:24:37.848829	005:00:47:51.615835	100's, 900's	yes
2011_01_04SOAR2_spcarch_1-47	2011	005:01:03:47.911138	005:19:08:38.324931	100's	yes
spc-20110105-120935_1-543	2011	005:20:11:19.018037	010:17:46:31.961513	100's	yes

CTP filename	Year	UTC Start Time	UTC Stop Time	CS-SVM: newer Hyds NOT Detected	CS-SVM on Legacy Hyds?
spc-20110110-095052_1-29	2011	010:17:52:39.757303	010:23:56:27.202858	100's	no
spc_LowFreq_10Jan1602L_1-8	2011	011:00:01:36.137996	011:01:40:07.946369	100's	no
spc_LowFreq_11Jan1021L_1-102	2011	011:18:34:40.455460	012:16:26:40.645263	100's	no
spc_LowFreq_12Jan10_1035L_1-1969	2011	012:18:39:38.637722	025:12:23:14.187743	100's	no
spc_LowFreq_01Feb11_1355L_1-47	2011	032:23:55:54.391379	033:15:10:09.686243	100's	no
spc_LowFreq_04Feb11_1007L_1-340	2011	035:18:08:00.594247	040:00:27:06.441965	100's	no
spc_LowFreq_08Feb11_1630L_1-733	2011	040:00:31:26.192808	048:15:30:25.592573	100's	no
spc_LowFreq_17Feb11_1101L_1-1570	2011	048:16:03:49.789789	067:12:09:28.665090	100's	no
Apr52011_1418_1-138	2011	095:21:18:21.244537	097:00:39:35.502601	100's	no
May192011_1406_1-3081	2011	139:21:06:29.520132	149:18:31:59.975676	100's	yes
SOAR_p5022_26July2011_1025z_1-7	2011	207:21:25:38.879467	207:22:15:05.434523	100's	yes
SOAR_p5022_26July2011_2315z_1-1272	2011	207:22:17:14.544407	214:16:04:05.737097	100's	yes
SOAR_p5022_2August2011_0905L_1-156	2011	214:16:07:50.939775	217:18:00:49.227443	100's	yes
SOAR_p5022_02August2011_1255l_1-1311	2011	214:19:55:43.171289	237:05:52:30.471041	100's	yes
SOAR_p5022_29August2011_1530l_1-1797	2011	241:22:28:12.644017	290:17:37:04.353836	100's	yes
SOAR_p5022_17Oct2011_1040l_1-1096	2011	290:17:39:25.707551	318:16:08:18.418664	100's	yes
p5022_23Nov2011_0736l_1-1838	2011	327:15:38:35.954590	008:21:00:19.671841	100's, 900's	yes
SOAR_p5022_10Jan2012_1313l_1-77	2012	010:21:14:44.328358	013:16:21:59.033558	100's, 900's	yes
SOAR_p5022_13Jan2012_1545l_1-237	2012	013:23:47:41.781149	018:18:35:13.550894	100's, 900's	yes
SOAR_p5022_18Jan2012_1426l_1-306	2012	018:22:27:02.758403	026:20:42:01.930567	100's, 600's, 700's	yes
SOAR_p5022_30Jan2012_1012_1-389	2012	030:18:13:00.775069	040:16:18:17.319202	100's, 600's, 700's	yes
SOAR_p5022_10Feb2012_0833l_1-840	2012	041:16:35:11.468781	054:14:03:39.852284	100's, 600's, 700's	yes
SOAR_p5022_13Mar2012_1521l_1-2244	2012	073:22:27:51.308660	133:19:14:23.549151	100's, 600's, 700's	no
SOAR_p5022_27July2012_1110l_204-322	2012	213:00:09:10.710697	214:20:11:08.882869	900's	no
SOAR_p5022_01Aug2012_1350l_1-111	2012	214:23:59:20.672316	216:23:04:33.167548	none	no
SOAR-p5022-15Oct2012-1039l_1-1148	2012	289:17:39:22.108743	307:10:55:27.233577	none	no
spc-20121114-223703_1-1405	2012	319:23:23:23.015602	329:03:18:45.669902	none	no
spc-20121209-031740_1-58	2012	344:04:02:28.762816	344:17:47:15.002085	100's	no
spc-20121209-162727_1-2094	2012	344:21:28:46.666847	352:07:21:17.262610	100's	no
spc-20130515-152432_1-434	2013	135:15:20:36.382107	141:02:03:04.060712	100's	no
spc-20130521-030611_1-74	2013	141:03:02:48.714621	141:18:17:09.560216	100's	no
20130521-182537_1-1822	2013	141:18:22:20.808568	189:21:36:21.903847	none	no
spc-20130708-232534_1-302	2013	189:23:10:05.777964	196:21:11:09.796475	none	no
spc-20130723-182715_1-1028	2013	204:18:10:41.525588	226:15:38:48.937309	none	no
spc-20130814-160438_1-5563	2013	226:15:49:08.758592	277:05:12:19.662379	none	no
spc-20131030-001657_1-665	2013	303:00:05:25.051527	306:22:07:29.215300	none	no

CTP filename	Year	UTC Start Time	UTC Stop Time	CS-SVM: newer Hyds NOT Detected	CS-SVM on Legacy Hyds?
spc-20131220-220220_1-2084	2013	354:22:53:16.865345	010:15:16:17.610566	none	no
spc-20140110-145356_1-31	2014	010:15:45:44.285907	010:20:49:37.260215	none	no
spc-20140110-200947_1-2590	2014	010:21:01:34.560020	037:17:33:03.618147	none	no
spc-20140207-184641_1-605	2014	038:18:20:29.876302	044:20:40:26.789456	none	no
spc-20140220-181938_1-953	2014	051:17:52:34.642879	062:21:53:42.832753	none	no
spc-20140306-193437_1-849	2014	066:00:33:39.615461	084:01:15:14.505858	none	no
spc-20140325-164102_1-14	2014	084:20:40:25.954482	085:04:31:12.370140	none	no
spc-20140327-110833_1-310	2014	086:15:08:17.508174	092:12:39:00.128002	none	no
spc-20140404-145129_1-1013	2014	094:18:50:56.801798	133:10:56:21.088286	none	no
spc-20140517-114710_1-2715	2014	137:15:47:29.861131	168:11:55:16.989616	none	no
spc-20140717-124800_1-905	2014	198:16:49:19.895327	203:16:49:04.894552	none	no
spc-20140722-134357_1-614	2014	203:17:46:11.352862	210:16:58:32.981048	none	no
spc-20140731-120345_1-7	2014	212:16:05:18.573339	212:17:33:25.240628	600's - 900's	no
spc-20140731-133519_1-179	2014	212:17:37:07.289253	214:17:05:16.213806	none	no
spc-20140802-145110_1-1120	2014	214:18:52:52.061505	224:12:32:52.067702	none	no
spc-20140827-150309_1-638	2014	239:19:05:15.402245	245:20:20:54.901881	600's - 900's	no
spc-20140905-164539_1-3184	2014	248:20:48:03.160131	287:06:04:40.569208	none	no
spc-20141128-165614_1-3455	2014	332:21:59:44.780333	003:15:18:40.865711	none	no
spc-20150103-101825_1-4670	2015	003:15:22:25.857544	056:23:14:12.217620	none	no
spc-20150225-182007_1-505	2015	056:23:25:01.377558	063:00:15:43.839118	none	no
spc-20150310-130533_1-179	2015	069:17:10:56.915078	071:21:31:06.622039	none	no
spc-20150313-154130_1-100	2015	072:19:46:22.483443	073:18:46:45.255079	none	no
spc-20150314-181842_1-185	2015	073:22:23:42.528440	075:17:12:02.791259	none	no
spc-20150316-135133_1-412	2015	075:17:56:34.180805	080:17:24:50.492868	none	no
spc-20150324-122008_1-718	2015	083:16:25:23.960904	091:11:45:06.953229	none	no
spc-20150407-124700_1-1993	2015	097:16:52:40.185896	118:17:18:37.548324	none	no
CTP_spc-20150428-151640_1-3406.txt	2015	118:19:22:23.469175	153:20:10:07.906300	none	no
CTP_spc-20150608-160130_1-483.txt	2015	159:20:07:32.837549	165:04:15:47.638394	700's	no
CTP_spc-20150624-134350_1-104.txt	2015	175:17:50:08.145385	176:21:55:26.379485	700's	no
CTP_spc-20150626-094305_1-51.txt	2015	177:13:49:26.288188	177:23:50:06.134422	700's	no
CTP_spc-20150627-101313_1-16.txt	2015	178:14:19:35.743193	178:18:26:22.430398	700's	no
CTP_spc-20150629-090903_1-35.txt	2015	180:13:15:18.645583	180:22:16:41.751570	700's	no
CTP_spc-20150701-091604_1-78.txt	2015	182:13:22:33.149661	182:22:25:55.015507	700's	no
CTP_spc-20150708-105855_1-681.txt	2015	189:15:06:19.293923	198:20:49:11.426753	700's	no
CTP_spc-20150717-195717_1-785.txt	2015	199:00:03:41.926995	204:13:53:02.526832	700's	no
CTP_spc-20150724-114209_1-422.txt	2015	205:15:49:15.555151	209:11:57:03.560848	700's	no
CTP_spc-20150811-112944_1-3558.txt	2015	223:15:37:36.133770	258:02:15:36.266369	none	no
CTP_spc-20151002-131605_1-4556.txt	2015	275:17:24:02.616805	319:06:51:29.109455	700's	no
CTP_spc-20151221-150800_1-3.txt	2015	355:20:16:40.614686	355:21:22:13.185789	700's	no

CTP filename	Year	UTC Start Time	UTC Stop Time	CS-SVM: newer Hyds NOT Detected	CS-SVM on Legacy Hyds?
CTP_spc-20151221-162528_1-1164.txt	2015	355:21:34:03.039650	005:18:42:06.271517	700's	no
CTP_spc-20160106-115919_1-2352.txt	2016	006:17:07:54.589506	040:18:48:05.883868	700's	no
CTP_spc-20160212-131900_1-669.txt	2016	043:18:27:54.258958	052:15:47:02.363692	700's	no
CTP_spc-20160221-122613_1-5419.txt	2016	052:17:35:21.255505	111:10:31:44.857610	none	no
CTP_spc-20160426-151309_1-1430.txt	2016	117:19:24:07.658952	130:22:08:21.034729	none	no
CTP_spc-20160523-160332_1-2295.txt	2016	144:20:15:10.725801	158:19:38:49.679151	none	no
CTP_spc-20160620-125146_1-9.txt	2016	172:17:03:20.008193	172:19:11:42.701775	none	no
CTP_spc-20160715-114136_1-8135.txt	2016	197:15:53:13.924452	268:19:04:16.277412	none	no
CTP_spc-20160926-173458_1-101.txt	2016	270:21:46:48.806099	271:12:50:38.085996	none	no
CTP_spc-20161104-171147_1-4773.txt	2016	309:21:24:25.037566	356:16:49:26.354867	none	no
CTP_spc-20161221-144946_1-2626.txt	2016	356:20:03:08.797218	014:21:38:15.070464	none	yes
CTP_spc-20170316-170837_1-2.txt	2017	075:21:24:46.782246	075:21:40:20.120366	none	no
CTP_spc-20170316-170946_1-2.txt	2017	075:21:25:21.649807	075:21:40:20.120366	none	no
CTP_spc-20170316-174208_1-2.txt	2017	075:21:57:49.070576	075:22:21:26.765245	none	no
CTP_spc-20170316-181220_1-2.txt	2017	075:22:27:51.991160	075:22:52:17.750999	none	no
CTP_spc-20170320-133249_1-2949.txt	2017	079:17:48:23.926297	104:23:11:30.408868	none	yes
CTP_spc-20170415-171743_1-16.txt	2017	105:17:17:58.662642	105:21:12:22.132557	none	yes
CTP_spc-20170415-235508_1-85.txt	2017	105:23:55:12.419846	106:19:14:12.560467	none	yes
CTP_spc-20170416-192514_1-1395.txt	2017	106:19:25:27.472305	122:12:01:47.230936	none	yes
CTP_spc-20170720-171727_1-6374.txt	2017	201:17:16:06.023655	258:15:43:20.640454	none	yes
CTP_spc-20170922-204255_1-3750.txt	2017	265:20:40:39.525392	290:19:15:20.188595	none	yes
CTP_spc-20171102-223528_1-2165.txt	2017	306:22:34:32.137905	325:12:52:36.407693	none	yes
CTP_spc-20171121-223641_1-2517.txt	2017	325:22:34:28.334537	344:20:04:03.029969	none	yes

Legacy/No Legacy issue samples

Missing Strings issue samples

**Table 30: SOAR Click Train Processor (CTP) files from 2010 to 2017.**